ELECTROSPINNING LECITHIN-POLYCAPROLACTONE SCAFFOLDS WITH GOLD NANOPARTICLES FOR OSTEOARTHRITIS PREVENTION

A thesis

presented to

the Faculty of the Graduate School

at the University of Missouri-Columbia

In Partial Fulfilment

Of the Requirements for the Degree

Master of Science

---

by

TONI CHRISTIAN MATSON

Dr. Sheila Grant, Thesis Supervisor

MAY 2018

The undersigned, appointed by the dean of the Graduate School, have examined the thesis entitled

ELECTROSPINNING LECITHIN-POLYCAPROLACTONE SCAFFOLDS WITH GOLD NANOPARTICLES FOR OSTEOARTHRITIS PREVENTION

presented by Toni Christian Matson,

a candidate for the degree of Master of Science,

and hereby certify that, in their opinion, it is worthy of acceptance.

_____
Dr. Sheila Grant

_____
Dr. Ferris Pfieffer

_____
Dr. Bret Ulery

DEDICATION

To my grandparents, Rick and Rosemary, your unwavering belief in me has pushed me to become the person that I am today. Thank you for inspiring confidence in me and continually supporting me in my education and teaching me what insurmountable love looks like.

ACKNOWLEDGMENTS

First, I would like to thank Dr. Sheila Grant for her acceptance, encouragement, and instruction throughout my undergraduate and graduate studies at Mizzou. Her passion and mentorship were the driving forces in my pursuit of a master's degree. Without her patience and understanding (and reviewing chapters), I never would have been able to complete this project. She continually pushed me to perform my best work and gave me the encouragement I needed to persevere.

I would also like to thank Mr. Dave Grant for his continued help in conducting experiments throughout my time in the Grant Lab. I would also like to thank him for his genuine interest in my future career and advice to make my dreams come true. His words of wisdom and never-ending optimism were vital in the completion of this project

Additionally, I would like to thank Dr. Ferris Pfeiffer and Dr. Bret Ulery for giving me feedback on my research, answering questions, and offering advice. Their time was very appreciated throughout my graduate studies

I am truly indebted to my "lab dad" Chris Glover. He was more than generous with his time showing me how to use the laboratory equipment, computer programs, and how to conduct experiments. He offered advice and answered questions I had at all hours of the day and has been a good friend. I also would like to thank all of my lab mates for providing support, guidance, advice, and a fun lab space.

Lastly, I would like to thank my friend and my college, Caio Peixoto. I never would have survived this year without his encouragement and support. He has

continually put my time over his own and has spent countless hours editing papers, critiquing presentations, and helping me make sense of data.

TABLE OF CONTENTS

LIST OF FIGURES

LIST OF TABLES

ABSTRACT

The human body has articular cartilage covering the ends of the bones to act as a shock absorber and aid in movement. In a disease state, this articular cartilage breaks down causing pain, swelling, and stiffness. With time, the cartilage continues to wear down, and bone on bone interactions occur. This disease is osteoarthritis (OA), and it is the most prevalent joint degenerative disease, affecting approximately 27 million Americans. OA cannot be reversed, so treatment methodologies are mostly palliative, which only provides temporary pain relief, or alternatively are very invasive, requiring total knee replacement.

To help mitigate the progression of OA, a hydrophilic, immunomodulatory membrane was developed, which would be placed over the articulating surface to prevent further degeneration of osteoarthritic cartilage. The electrospun membrane is composed of 20 nm gold nanoparticles, soy lecithin, and the polymer polycaprolactone (PCL). Soy lecithin and PCL solutions were electrospun to develop a unique nonwoven mat for OA. The electrospinning parameters were optimized to achieve different solution ratios for the best fiber formation. Different concentrations of lecithin and PCL were used: the amount of solute needed was 40% (w/v) and the amount of lecithin mixed with PCL was 40% (40:40), and 50% (w/v) solute needed with 50% soy lecithin with PCL (50:50). 20 nm gold nanoparticles were then introduced at 1%, 5%, and 10% (v/v) to modulate the inflammatory response.

The chemical composition of the scaffolds was analyzed via Fourier Transform Infrared Spectroscopy (FTIR), and the thermal properties were investigated using

Differential Scanning Calorimetry (DSC) and Thermogravimetric Analysis (TGA) to determine stability and percent of materials. Contact Angle Measurements were taken to observe the hydrophilicity of the scaffolds. Neutron Activation Analysis (NAA) was performed to quantify the gold nanoparticles present in the mats. Scanning Electron Microscopy (SEM) was conducted to determine fiber formation as well as nanoparticle presence. To characterize the biocompatibility and cytotoxicity of the mats, WST-1 and ROS assays were performed using L929 murine fibroblast cells.

It is expected that lecithin and gold will be homogeneously integrated with the PCL and that the mechanical properties will be strong enough to withstand the microenvironment of the knee. This study demonstrated that it is possible to successfully electrospin lecithin and polycaprolactone nanofibrous scaffolds with various polymerized solution concentrations with and without gold nanoparticles. It was hypothesized that the electrospun lecithin/PCL/nanoparticle scaffold would promote hydrophilicity while maintaining strength and flexibility, thereby prolonging mechanical stability in cartilage

1. Literature Review

1.1 Introduction to Osteoarthritis

Of any joint disease, osteoarthritis (OA) of the knee affects the most people. It affects approximately 27 million Americans [1] or 10% of men and 18% of women over the age of 60 [2]. It is unknown why exactly it presents more in women than men, but it is hypothesized to do with multiple factors such as hormones, previous trauma, and anatomical differences [3]. This degenerative joint disease occurs most often in the elderly, but it can happen earlier in athletic people due to trauma [4]. Standard joints have healthy cartilage covering the end of each bone to provide a slippery, gliding surface to assist in joint motion. The primary purpose of articular cartilage is to act as a shock absorber between the bones. Patients with osteoarthritis experience pain, swelling, and stiffness in their joints due to cartilage breakdown. As the disease worsens with time, and the cartilage continues to wear down, it may break away and float around in the joint. Bone may also chip away once the cartilage is gone and bone on bone interactions will

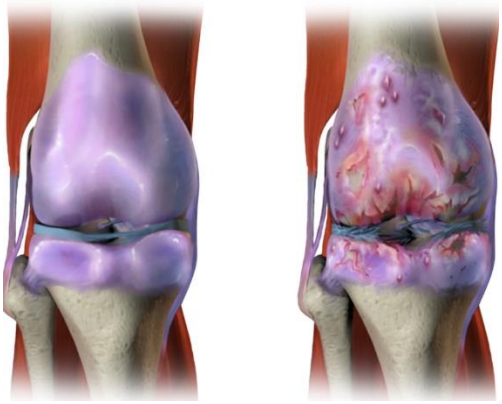

Figure 1.1 Comparison of a healthy knee joint (left) and an osteoarthritic knee joint (right). Cartilage begins to crack and break down. The meniscus will slowly erode, and bone spurs will form [6].

occur, leading to painful bone spurs. In the final stages of OA, the bones are left with little protection, resulting in permanent joint damage and even more pain [5]. Figure 1.1 shows a comparison of a healthy knee joint and an osteoarthritic knee joint.

Currently, there is no reversal of osteoarthritis due to the complex structure of the articular cartilage. Lesions in the cartilage heal poorly because of its avascular nature. It also has limited access to chondrocytes, the reparative cells in the cartilage, and growth factors [6]. It is for this reason that the structure of the cartilage must stay intact. Human cartilage is between 2 mm and 4 mm thick and is composed of water, collagen, and proteoglycans in a dense extracellular matrix (ECM) [7]. Within this structure, there are different zones – the superficial zone, the middle zone, the deep zone, and the calcified zone – and each zone has three regions – the pericellular region, the territorial region, and the interterritorial region – making it extremely difficult to replicate [7]. Figure 1.2 shows a cross-section of articular cartilage.

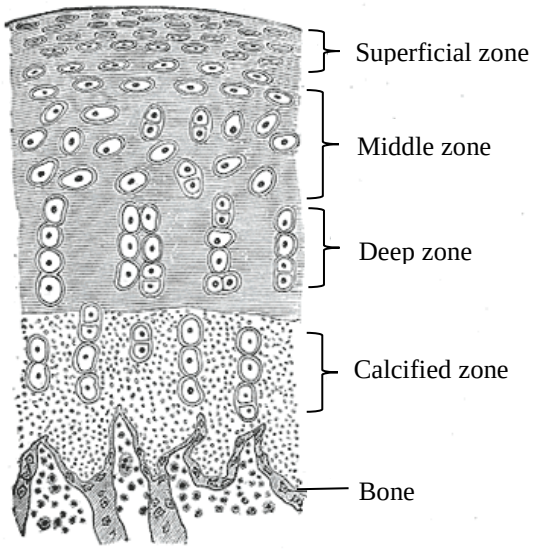

Figure 1.2 A cross section of articular cartilage is shown. Articular cartilage has 4 layers: the superficial zone, the middle zone, the deep zone, and the calcified zone. Each of these zones have three separate regions, making articular cartilage extremely hard to replicate [9].

Exercising and achieving a healthy BMI can help manage symptoms of osteoarthritis along with physical therapies and anti-inflammatory medication. If conservative treatments do not work, several procedures are currently performed such as cortisone injections, lubrication injections, realignment surgery, and as a last resort, joint replacement [8]. Cortisone shots are injected directly into the knee joint to lower inflammation. This injection relieves joint pain, but patients must continue receiving them for relief. The duration of time for pain relief varies by patient, and some patients do not experience any comfort [9]. There is even concern that too many injections will cause the cartilage to degenerate further [8]. For lubrication injections, hyaluronic acid is administered because it is the natural fluid in the knee. This injection provides some cushioning to lower inflammation, but there is debate over the efficacy of this method. Arrich *et al.* [10] suggest in a review article, these injections might only provide the same level of relief as placebos. If OA has damaged only one side of the knee, an osteotomy could be helpful. This procedure allows a surgeon to add or remove a wedge of bone to offer relief to the damaged part of the knee [8].

The final option is total joint arthroplasty, where the injured surfaces are shaved away and replaced with a prosthesis composed of plastic, usually ultra-high molecular weight polyethylene, and metal, usually cobalt-chromium or titanium. This surgery can lead to infections or blood clots, nerve injury, and the polyethylene spacer will often wear out due to friction and come loose with time, resulting in a revision surgery [11]**.** There are revision rates of 6% after five years and 12% after ten years [12], and 44% of revision surgeries are due to polyethylene wear [13].

The goal of this study is to create a membrane to act as a reinforcing material in the knee to prolong the natural joint. It would be placed over the articulating surface using minimally invasive surgery and would lessen the degeneration of the articular cartilage. This option will delay the need for a total knee replacement, eliminating the need for revision surgeries due to wear. It is superior to injections because it has longevity, and it prevents the cartilage from breaking down further, which keeps inflammation down, therefore allowing for pain relief.

1.2 Introduction to Electrospinning

The purpose of a tissue-engineered scaffold is to mimic the natural extracellular matrix (ECM) to enhance cell migration, proliferation, and adhesion to foster tissue growth [14]. The ideal properties are biocompatibility, high surface area, suitable surface chemistry, interconnected porosity, and mechanical properties close to the surrounding native tissue [15]. There are many different techniques to fabricate these scaffolds, one such technique is electrospinning.

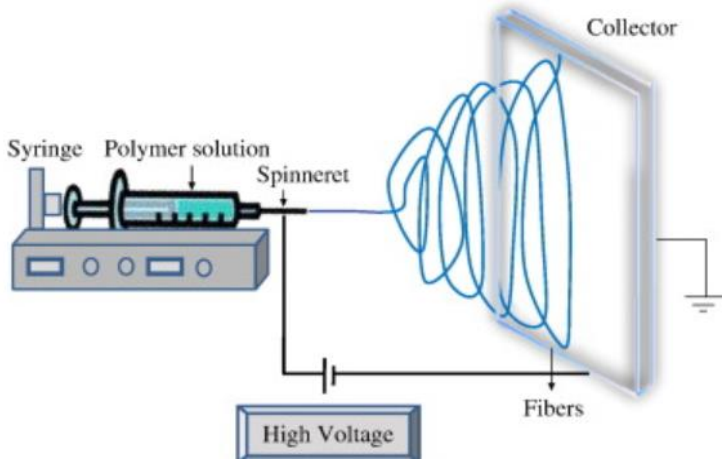

Figure 1.3 [20] Electrospinning can be used to create variously sized nanofibers by applying an electric field to attract a polymer melt utilizing the apparatus shown above.

Electrospinning is often used to create nanofibers because it is a quick and cost-effective method, increases surface area, creates porous scaffolds, and best mimics the ECM; meeting many of the requirements for a suitable scaffold [16]. Electrospun scaffolds are being used for bone, cardiovascular, and cartilage tissue [17], making this method an ideal way to produce the knee membranes for this study. The setup of a typical electrospinning apparatus (Figure 1.3) involves three major components: a high voltage power supply, a metallic needle, and a grounded collecting.

The metallic needle is attached to a syringe that holds a highly viscous polymer solution, sometimes known as the melt. A syringe pump pushes the solution at a steady and controlled rate. A high voltage (between 10-30 kV [18]) is applied to draw the melt to the plate. The voltage causes the drop at the end of the needle to become positively charged over the surface. These charges are attracted to the negatively charged collecting plate which will cause the droplet to distort into what is known as a Taylor cone. When the electrostatic force overcomes the surface tension, the droplet elongates, and shoots from the needle to the collecting plate. As the polymer is stretched, the solvent evaporates leading to the development of nonwoven (randomly-oriented) fibers on the collector [19]. A rotating mandrel with specific rotations per minute can be used to control the orientation of the nanofibers.

Many parameters affect the final electrospun material, and they must be optimized for generation of homogenous nanofibers. If any of the settings are out of place, the surface will have a different outcome. These parameters are split into three different categories: solution parameters, process parameters, and environmental parameters [20]. The solution parameters are polymer concentration, polymer molecular weight, viscosity,

and surface tension. These all work together to create smooth nanofibers. If the concentration is too low, it will result in lower viscosity and electrospraying will occur instead of electrospinning. If there is a fixed concentration and the molecular weight is too small, beads will form [21].

Process parameters are those that are controllable: voltage, working distance from the needle tip to the collecting plate, and flow rate of the solution. If the working distance is too short and the flow rate is too fast, the fibers will not be able to polymerize completely. Additionally, having a flow rate that is too high will also result in thick fibers morphed together because they had a short drying time. If the working distance is too long, it will also result in beading on the fibers [21].

The environmental parameters are temperature and humidity, and without an environmentally-controlled chamber, these are uncontrollable. If the humidity is too high, it will cause the stretching force to be minimal, and it can result in pores on the fibers themselves. The formation of the pores is due to condensation on the fibers during the electrospinning process [22].

1.3 Introduction to Scaffold Materials

Polycaprolactone (PCL) was selected for this project because it is an FDA approved biodegradable, biocompatible polymer with acceptable material properties [23]. Biocompatibility, as defined by D.F.Williams, is "ability to perform with an appropriate host response in a specific application [24]." In this case, it would mean that the polymer has nontoxic byproducts, does not induce excessive inflammation or immunogenic response, and does not create blood clots [25].

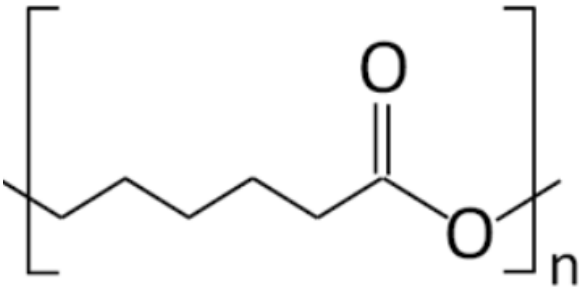

Figure 1.4 The ester linkages of the PCL structure allow for hydrolysis of the polymer under normal physiological conditions of the body [29].

The structure of PCL can be seen in Figure 1.4 to have repeating units of a five-member hydrocarbon chain bound to an ester moiety [26]. PCL is a semicrystalline thermoplastic, so it is more flexible above its glass transition temperature (T_g). PCL has a relatively low T_g of -60º C, meaning it becomes very flexible when placed *in vivo*, making it harder to tear in a dynamic environment [27]. The polymer will begin melting at 60º C, which is much lower than that of the human body at 37º C [28]. With a melting temperature (T_m) that is much higher than body temperature, premature degradation of the material will not be a concern. Once in the body, it is degraded through nonenzymic hydrolysis, meaning water attacks the carbonyl group of the ester and it is cleaved. Once the ester group is cleaved, an alcohol and a carboxylic acid remain. The body can process these groups, and they are excreted, showing that the byproducts are non-toxic [29]. It takes approximately two years to completely degrade, allowing for proper tissue regrowth [30]. Biomedical applications for PCL include drug delivery systems, wound healing, and tissue engineering scaffolds for vascular grafts, skin regeneration, bone regrowth, and cartilage repair [23]. It is essential for scaffolds to have a hydrophilic surface with high surface area to better promote the embedding and proliferation of cells. Unfortunately,

PCL is hydrophobic leading to reduced cell affinity and adhesion, requiring some surface modifications [15].

Soy lecithin is incorporated into solution before electrospinning to improve the hydrophobic property of PCL. Soy lecithin is composed of naturally occurring phospholipids, extracted from soybean oil. Lecithin is widely used in the food industry and is not harmful to the body; some even take it as a supplement to treat cholesterol [31] and improve immune function [32]. Lecithin molecules are amphiphilic, so they have a lipid molecular structure possessing a charged head group and a hydrocarbon tail. Due to the amphiphilic structure, lecithin can act as a surfactant and create a hydrophilic surface [33].

Zhang et al. [33] showed that the incorporation of lecithin to PCL increases hemocompatibility (biocompatibility of blood), lowers protein adsorption due to improved hydrophilicity, enhances cell growth, and decreases inflammatory response. It is reasonable to theorize that mixing lecithin in solution modifies the surface physiochemical performance of PCL, which can lead to a more optimal microenvironment for tissue regeneration.

Coverdale et al. [34] also incorporated lecithin into electrospun PCL scaffolds to lower the hydrophobicity of the polymer. This study found that the blended mats drastically reduced hydrophobicity, but also resulted in increased biocompatibility, and enhanced the efficiency of cell-seeding. Since the lecithin is mixed in the solution, these improved properties are considered bulk characteristics and are not isolated to the surface, so the improvements continue throughout the degradation of the scaffold. As the PCL degrades, the lecithin will slowly cleave off of the membrane. The body breaks

lecithin into choline and the phospholipid components and metabolizes them [35]. The phospholipid components: phosphate, glycerol, and fatty acids can be seen in Figure 1.5.

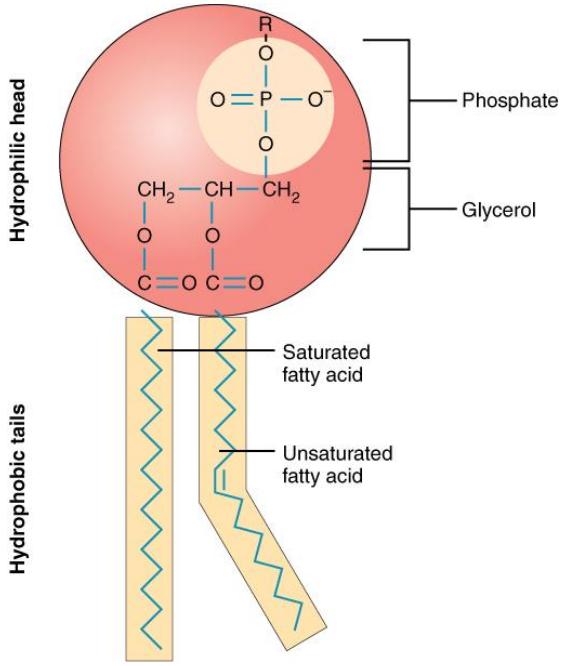

Figure 1.5 Soy lecithin is composed of naturally occurring phospholipids. Phospholipids have a hydrophilic head group and a hydrophobic tail. Upon degradation, lecithin breaks down into choline, phosphate, glycerol, and fatty acids. The body then metabolizes these components [38].

Gold nanoparticles (AuNPs), solid gold colloidal particles, have been gaining a lot of interest in nanomedicine and are used in drug delivery, cell imaging, stem cell tracking, and nanocomposite scaffolds [36]. The addition of AuNPs to mats has shown to improve mechanical and adhesive properties, which creates an ideal microenvironment to allow regeneration of damaged tissue [14]. AuNPs also show antioxidant properties [37], so inflammation will be lowered. The versatility of size and surface chemistry can attribute to the widespread use of AuNPs. This study will incorporate 20 nm AuNPs into the PCL/lecithin blend to enhance the efficacy of the scaffold.

The PCL/lecithin/gold blend has the potential to be superior to other scaffolds because the degradation time is much slower than hydrogels and other polymers, minimizing the number of procedures the patient must undergo.

1.4 References

[1] "NIH Fact Sheets - Osteoarthritis." [Online]. Available: https://report.nih.gov/nihfactsheets/ViewFactSheet.aspx?csid=55. [Accessed: 06-Mar-2018].

[2] S. Glyn-Jones *et al.*, "Osteoarthritis," *The Lancet*, vol. 386, no. 9991, pp. 376–387, Jul. 2015.

[3] S. L. Hame and R. A. Alexander, "Knee osteoarthritis in women," *Curr. Rev. Musculoskelet. Med.*, vol. 6, no. 2, pp. 182–187, Mar. 2013.

[4] D. R. Leung, "Osteoarthritis of the knee," *InnovAiT*, p. 1755738017753455, Mar. 2018.

[5] "What is Osteoarthritis?," *arthritis.org*. [Online]. Available: http://www.arthritis.org/about-arthritis/types/osteoarthritis/what-is-osteoarthritis.php. [Accessed: 14-Mar-2018].

[6] J. Fitzgerald, "Enhanced cartilage repair in 'healer' mice—New leads in the search for better clinical options for cartilage repair," *Semin. Cell Dev. Biol.*, vol. 62, pp. 78–85, Feb. 2017.

[7] A. J. Sophia Fox, A. Bedi, and S. A. Rodeo, "The Basic Science of Articular Cartilage," *Sports Health*, vol. 1, no. 6, pp. 461–468, Nov. 2009.

[8] "Osteoarthritis - Diagnosis and treatment - Mayo Clinic." [Online]. Available: https://www.mayoclinic.org/diseases-conditions/osteoarthritis/diagnosis-treatment/drc-20351930. [Accessed: 14-Mar-2018].

[9] B. Arroll and F. Goodyear-Smith, "Corticosteroid injections for osteoarthritis of the knee: meta-analysis," *BMJ*, vol. 328, no. 7444, p. 869, Apr. 2004.

[10] J. Arrich, F. Piribauer, P. Mad, D. Schmid, K. Klaushofer, and M. Müllner, "Intra-articular hyaluronic acid for the treatment of osteoarthritis of the knee: systematic review and meta-analysis," *CMAJ Can. Med. Assoc. J. J. Assoc. Medicale Can.*, vol. 172, no. 8, pp. 1039–1043, Apr. 2005.

[11] W. L. Healy *et al.*, "Complications of total knee arthroplasty: standardized list and definitions of the Knee Society," *Clin. Orthop.*, vol. 471, no. 1, pp. 215–220, Jan. 2013.

[12] G. Labek, M. Thaler, W. Janda, M. Agreiter, and B. Stöckl, "Revision rates after total joint replacement," *J. Bone Joint Surg. Br.*, vol. 93-B, no. 3, pp. 293–297, Mar. 2011.

[13] K. T. Kim, S. Lee, D. O. Ko, B. S. Seo, W. S. Jung, and B. K. Chang, “Causes of Failure after Total Knee Arthroplasty in Osteoarthritis Patients 55 Years of Age or Younger,” *Knee Surg. Relat. Res.*, vol. 26, no. 1, pp. 13–19, Mar. 2014.

[14] S. Vial, R. L. Reis, and J. M. Oliveira, “Recent advances using gold nanoparticles as a promising multimodal tool for tissue engineering and regenerative medicine,” *Curr. Opin. Solid State Mater. Sci.*, vol. 21, no. 2, pp. 92–112, Apr. 2017.

[15] I. Rajzer, E. Menaszek, and O. Castano, “Electrospun polymer scaffolds modified with drugs for tissue engineering,” *Mater. Sci. Eng. C*, vol. 77, no. Supplement C, pp. 493–499, Aug. 2017.

[16] V. Beachley and X. Wen, “Effect of electrospinning parameters on the nanofiber diameter and length,” *Mater. Sci. Eng. C*, vol. 29, no. 3, pp. 663–668, Apr. 2009.

[17] M. A. Woodruff and D. W. Hutmacher, “The return of a forgotten polymer—Polycaprolactone in the 21st century,” *Prog. Polym. Sci.*, vol. 35, no. 10, pp. 1217–1256, Oct. 2010.

[18] D. Li and Y. Xia, “Electrospinning of Nanofibers: Reinventing the Wheel?,” *Adv. Mater.*, vol. 16, no. 14, pp. 1151–1170, Jul. 2004.

[19] K. Garg and G. L. Bowlin, “Electrospinning jets and nanofibrous structures,” *Biomicrofluidics*, vol. 5, no. 1, p. 13403, Mar. 2011.

[20] M. Borrotti, E. Lanzarone, F. Manganini, S. Ortelli, A. Pievatolo, and C. Tonetti, “Defect minimization and feature control in electrospinning through design of experiments,” *J. Appl. Polym. Sci.*, vol. 134, no. 17, p. n/a-n/a, May 2017.

[21] Z. Li and C. Wang, “Effects of Working Parameters on Electrospinning,” 2013, pp. 15–28.

[22] S. Megelski, J. S. Stephens, D. B. Chase, and J. F. Rabolt, “Micro- and Nanostructured Surface Morphology on Electrospun Polymer Fibers,” *Macromolecules*, vol. 35, no. 22, pp. 8456–8466, Oct. 2002.

[23] S. Reyes Lopez, D. Cornejo-Monroy, and G. Gonzalez, “A Novel Route for the Preparation of Gold Nanoparticles in Polycaprolactone Nanofibers,” *J. Nanomater.*, vol. 2015, Apr. 2015.

[24] D. F. Williams, “A model for biocompatibility and its evaluation,” *J. Biomed. Eng.*, vol. 11, no. 3, pp. 185–191, May 1989.

[25] E. W. Lau, “11 - Leads and Electrodes for Cardiac Implantable Electronic Devices,” in *Clinical Cardiac Pacing, Defibrillation and Resynchronization Therapy (Fifth Edition)*, Elsevier, 2017, pp. 313-351.e29.

[26] M. Abedalwafa, F. Wang, L. Wang, and C. Li, “Biodegradable Poly-epsilon-caprolactone (PCL) for Tissue Engineering Applications: A Review,” *Rev Adv Mater Sci*, vol. 34, pp. 123–140, 2013.

[27] C. A. Harper, Ed., *Modern plastics handbook*. New York: McGraw-Hill, 2000.

[23] Morrison SF. Regulation of body temperature. In: Boron WF, Boulpaep EL, eds. Medical Physiology. 3rd ed. Philadelphia, PA: Elsevier; 2017:chap 59.

[29] A. Mahapatro and D. Singh, *Biodegradable Nanoparticles are Excellent Vehicle for Site Directed in-vivo Delivery of Drugs and Vaccines*, vol. 9. 2011.

[30] E. Diaz, I. Sandonis, and M. Blanca Valle, *In Vitro Degradation of Poly(caprolactone)/nHA Composites*, vol. 2014. 2014.

[31] A. M. Mourad, E. de Carvalho Pincinato, P. G. Mazzola, M. Sabha, and P. Moriel, “Influence of Soy Lecithin Administration on Hypercholesterolemia,” *Cholesterol*, 2010.

[32] D. T. S. Z. Miranda *et al.*, “Soy lecithin supplementation alters macrophage phagocytosis and lymphocyte response to concanavalin A: a study in alloxan-induced diabetic rats,” *Cell Biochem. Funct.*, vol. 26, no. 8, pp. 859–865, Dec. 2008.

[33] M. Zhang, K. Wang, Z. Wang, B. Xing, Q. Zhao, and D. Kong, “Small-diameter tissue engineered vascular graft made of electrospun PCL/lecithin blend,” *J. Mater. Sci. Mater. Med.*, vol. 23, no. 11, pp. 2639–2648, Nov. 2012.

[34] B. D. M. Coverdale, J. E. Gough, W. W. Sampson, and J. A. Hoyland, “Use of lecithin to control fiber morphology in electrospun poly (ε-caprolactone) scaffolds for improved tissue engineering applications,” *J. Biomed. Mater. Res. A*, vol. 105, no. 10, pp. 2865–2874, Oct. 2017.

[35] N. Garti and A. Aserin, “12 - Effect of Emulsifiers on Cocoa Butter and Chocolate Rheology, Polymorphism, and Bloom,” in *Cocoa Butter and Related Compounds*, AOCS Press, 2012, pp. 275–305.

[36] S. van Rijt and P. Habibovic, “Enhancing regenerative approaches with nanoparticles,” *J. R. Soc. Interface*, vol. 14, no. 129, Apr. 2017.

[37] A. Rajan, V. Vilas, and D. Philip, “Studies on catalytic, antioxidant, antibacterial and anticancer activities of biogenic gold nanoparticles,” *J. Mol. Liq.*, vol. 212, pp. 331–339, Dec. 2015.

2. Introduction to Research

2.1 Significance of Research

The primary application being investigated in this study is the development of a scaffold to delay the progression of articular cartilage degeneration. Cartilage regeneration is a primary focus in tissue engineering because of the increasing prevalence of arthritis and other cartilage damage. As stated previously, cartilage is unable to heal itself once severely damaged. It is projected that by 2040, 78.4 million adults will have doctor-diagnosed arthritis, a 49% increase [1]. There is a substantial economic burden in managing osteoarthritis, even before undergoing a total knee replacement [2]. The scaffold in this research is designed primarily for knee joints, but it could be utilized in any joint with articular cartilage. The scaffold will be fixated over the articular surface and remain intact for approximately two years, reducing the progression of articular cartilage degradation. It may be possible that during this two-year period, tissue regeneration may occur.

2.2 Research Objectives

The overall goal of this project is to create a hybrid polymer scaffold, via electrospinning, that can be fixated on knee joints to slow the progression of cartilage degeneration. Scaffolds will be spun with different concentrations of polycaprolactone (PCL), lecithin, and gold nanoparticles (AuNPs) to optimize the properties of each component. A decision will be made on which design is superior for use *in vitro* before moving on to further testing. This project will examine three primary objectives:

Objective 1: Optimize electrospinning parameters to achieve homogenous mats with varying concentrations of PCL, soy lecithin, and 20 nm AuNPs.

- We hypothesize smooth and homogenous nonwoven scaffolds will be used as a reinforcing material for chondral defects in the knee.
- This objective will be reached by adjusting the electrospinning parameters one at a time until the scaffolds appear homogenous to the naked eye.

Objective 2: Characterize each scaffold to determine which solution ratio is best for attachment. Bulk and surface characteristics will be examined with pristine PCL as a control.

- We hypothesize that the lecithin and gold nanoparticles will improve characteristic properties without weakening structural integrity.
- We will perform contact angle measurements to ensure the lecithin lowers hydrophobicity; Fourier Transform Infrared Spectroscopy to ensure the lecithin has been integrated with PCL into the fiber scaffold and the solvents have evaporated out; Scanning Electron Microscopy to assess fiber diameter and AuNP presence; Differential Scanning Calorimetry will be used to evaluate the melting temperature of the scaffolds; and Thermogravimetric Analysis (TGA) will be performed to determine the degradation temperature of the scaffolds.

Objective 3: Characterize biocompatibility and cytotoxicity of scaffolds.

- We hypothesize that the incorporation of lecithin and gold nanoparticles will improve scaffold surface area, leading to better cell attachment and lower inflammation.
- A WST-1 assay will be performed to determine cell viability on the scaffolds.
- A reactive oxygen species (ROS) assay will show the biocompatibility of the scaffolds.

2.3 Research Design

The experiments performed for this project include seven experimental groups, which can be seen in Table 2.1. Sample concentrations and electrospinning parameters were based on previously successful experiments by Jonathan Gootee [3]. Each sample was prepared using the same protocol so there would be no discrepancies in fabrication. Pristine PCL is used as a control.

Table 2.1 Seven different sample types (Pristine PCL, 40:40, 50:50, 1% AuNP, 5% AuNP, 10% AuNP, and 50:50 with 10% AuNP) will be compared to one another

Pristine PCL	1% (v/v) AuNP, 0.2 g lecithin	50% (w/v) solute, 50% (w/w) lecithin, 10% (v/v) AuNP
40% (w/v) solute, 40% (w/w) lecithin	5% (v/v) AuNP, 0.2 g lecithin	
50% (w/v) solute, 50% (w/w) lecithin	10% (v/v) AuNP 0.2 g lecithin	

2.4 References

[1] J. M. Hootman, C. G. Helmick, K. E. Barbour, K. A. Theis, and M. A. Boring, "Updated Projected Prevalence of Self-Reported Doctor-Diagnosed Arthritis and Arthritis-Attributable Activity Limitation Among US Adults, 2015-2040," *Arthritis Rheumatol. Hoboken NJ*, vol. 68, no. 7, pp. 1582–1587, 2016.

[2] D. J. Hunter, D. Schofield, and E. Callander, "The individual and socioeconomic impact of osteoarthritis," *Nat. Rev. Rheumatol.*, vol. 10, no. 7, pp. 437–441, Jul. 2014.

[3] J. Gootee, E. Buettman, D. Grant, and S. Grant, "Fabrication and Characterization of an Electrospun PL and Soy Lecithin Composite Material," University of Missouri, 2016.

3. Scaffold Preparation

3.1 Preparing the solution

To create the viscous solution, low molecular weight poly- ε-caprolactone (PCL) (Sigma Aldrich, St. Louis, MO) and soy lecithin (Fearn Natural Foods, Mequon, WI) are measured based on the desired concentration and placed in a 20 mL beaker. The solute is mixed with a 5 mL solution of a 7:3 ratio of Dimethylformamide (DMF) (Sigma Aldrich, St. Louis, MO**)** and Chloroform ($CHCl_3$) **(**Fisher Chemical, Fair Lawn, NJ**)**. Pipette tips were replaced after each use to avoid cross-contamination. It is important to note that during the electrospinning process the solvents evaporate out, so these scaffolds are nontoxic, and solvents do not enter the bloodstream. This solution is sealed with Parafilm (Bemis, Chicago, IL) to ensure the solvents did not evaporate while on the stir plate and stirred at 200 rpm and 50 °C for two hours until the PCL is completely dissolved. The contents of the beaker on the stir plate can be seen in Figure 3.1.

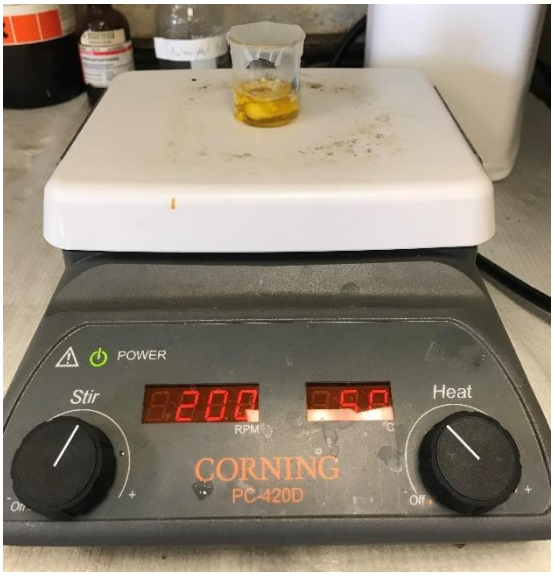

Figure 3.1 The 20 mL beaker contains PCL, lecithin, and AuNPs. This solution is stirred at 200 rpm and heated to 50 ºC for two hours, until the PCL is wholly dissolved.

It has been discovered by Gootee [1] that the concentrations that best avoid solution drips are 40:40 and 50:50. 40% concentration of solute (lecithin and PCL) in solvent solution (weight/volume %) and 40% concentration of lecithin in solute (weight %). 50% concentration of solute in solvent solution and 50% concentration of lecithin in solute. The calculations are based on Gootee's protocol [1], and are as follows:

40% Solute, 40% Lecithin (Solute includes both lecithin and PCL)

Solute needed: 5 mL (total solution) * 40% = 2 grams

Amount of lecithin: 2 grams * 40% = 0.8 grams (40% lecithin is required)

Amount of PCL: 2 grams – 0.8 grams = 1.2 grams (60% PCL is required to total solute to 100% (40% lecithin + 60% PCL))

Amount of $CHCl_3$ (chloroform): 3.5 mL

Amount of DMF (Dimethylformamide): 1.5 mL

50% Solute, 50% Lecithin (Solute includes both lecithin and PCL)

Solute needed: 5 mL (total solution) * 50% = 2.5 grams

Amount of lecithin: 2.5 grams * 50% = 1.25 grams (50% lecithin is required)

Amount of PCL: 2 grams – 1.25 grams = 1.25 grams (50% PCL is required to total solute to 100% (50% lecithin + 50% PCL))

Amount of $CHCl_3$ (chloroform): 3.5 mL

Amount of DMF (Dimethylformamide): 1.5 mL

In some samples, 20 nm gold nanoparticles (Ted Pella, Redding, CA) were introduced to the solution. Before adding the AuNP to the mixture, the colloid must be removed so there is no water separation. The desired volume was placed in a Jouan B4i Multifunction Centrifuge for 7.5 minutes at 12,500 rpm. The colloid was removed, and the nanoparticles were reconstituted with DMF to allow the solution to mix homogeneously. They were then added to the solution beaker before stirring.

3.2 Electrospinning Parameters and Process

When the solution appeared to be homogeneously mixed (after two hours), the beaker is removed from the stir plate, and the solution in the beaker is drawn into a 5 mL Luer-Lok syringe with an 18-gauge blunt needle. The parameters for the electrospinning apparatus have been previously determined to be 20 cm working distance from the end of the needle to the ground plate, 18 kV applied voltage, and a 6mL/hr flow rate [1]. There should be 15% humidity and approximately 22 ºC ambient temperature for best results. A syringe pump pushed the solution at a controlled rate through 48 cm of Tygon tubing, a rectangle of aluminum foil was attached to the ground plate to collect the nanofibers. The electrospinning set up has a horizontal orientation so if any of the polymer drips, it does not fall onto the scaffold. It is important to note that the box surrounding the electrospinning apparatus must be closed or the voltage will not be induced. If the door is opened at any time, an open circuit will occur to prevent electric shock. Figure 3.2 shows the electrospinning set up used for all experiments. The polymer droplet will become charged, and a Taylor cone forms, the polymer jet protruding from the cone is visible.

This phenomenon can be seen in Figure 3.3. Between 2 and 4 mL of solution was electrospun to generate a scaffold with a thickness that best represents the superficial layer of cartilage. When the spin was complete, the foil was carefully removed, labeled and stored. The result of a 40:40 scaffold can be seen in Figure 3.4.

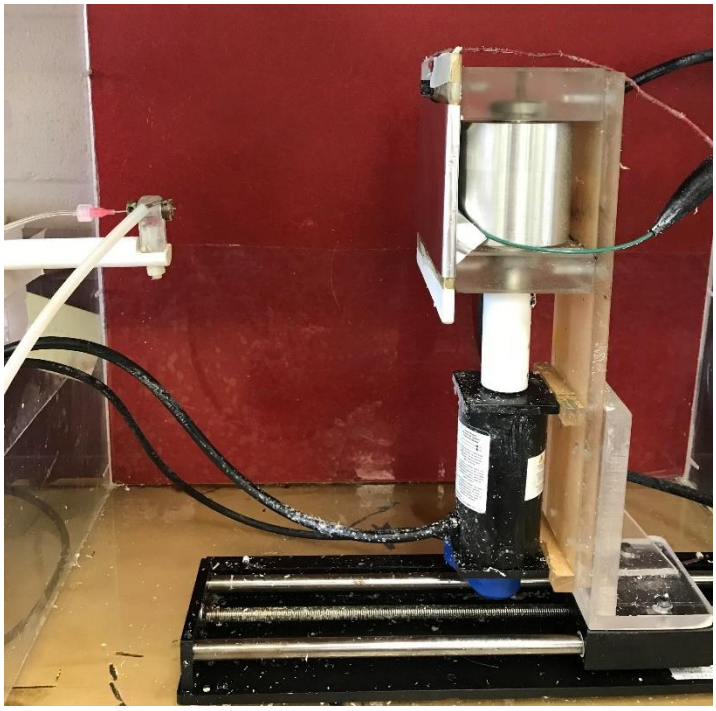

Figure 3.2 A horizontal orientation is used for the elector spinning set up so if any polymer drips, it does not fall on the scaffold. The needle tip and the collecting plate are shown, the high voltage supply

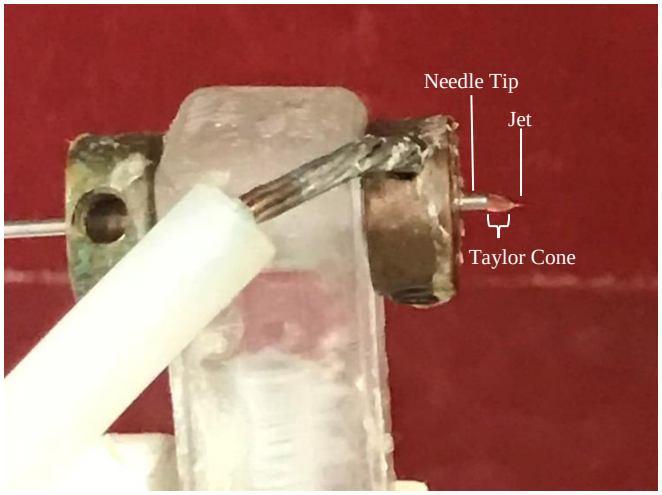

Figure 3.3 The electric field creates a Taylor cone by charging the polymer droplet. Once the surface tension is overcome, the jet races toward the collecting plate.

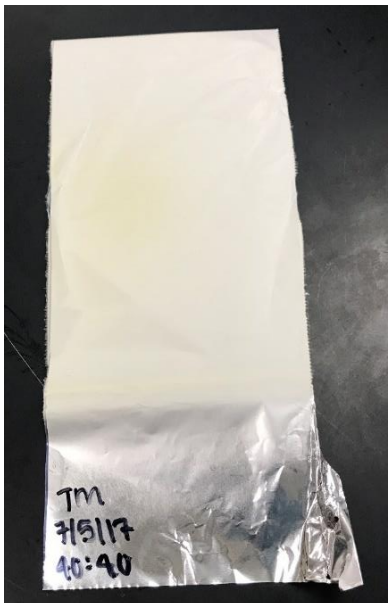

Figure 3.4 If the electrospinning parameters are optimal, a smooth homogeneous surface is produced. An electrospun 40:40 sample is shown.

3.3 Sterilization of Scaffolds

To accurately analyze the biocompatibility and cytotoxicity of the scaffolds, they must be sterilized. Several methods can be utilized to sterilize PCL scaffolds such as heat treatment, gamma irradiation, or chemical immersion [2]. The sterilization method used

for this project used a protocol involving immersion in peracetic acid. Since PCL degrades so slowly, it can stay immersed in the solution for an extended period without altering its chemical composition or compromising its structural integrity.

Each sample type was prepared by creating 4.5 mm punches (n=10) of each experimental group. A 0.1% (v/v) peracetic acid sterilization solution was prepared, and the pH was adjusted to ~7 by adding 1N NaOH. Under the sterile biological hood, the solution was filtered into a 1L unit with a .22 µm filter. The punches of each sample type were placed into their own sterile 125 mL flask, and 50 mL of the sterilization solution was pipetted on top of the samples. Caution was taken not to contaminate any tips, which would lead to the contamination of the scaffold samples. The flasks were placed on the orbital shaker at 225 rpm for 30 minutes. After this 30-minute incubation period, the sterilization solution was removed, and samples were placed into new 125 mL flasks. 50 mL of PBS solution was added to the flasks and put on the orbital shaker for 24 hours at 225 rpm. Two more PBS washes were performed for 24-hour periods to ensure there is no acidic residue, completing the sterilization process. The samples were immediately used in a cell study.

3.4 References

[1] J. Gootee, E. Buettman, D. Grant, and S. Grant, “Fabrication and Characterization of an Electrospun PL and Soy Lecithin Composite Material,” University of Missouri, 2016.

[2] Z. Dai, J. Ronholm, Y. Tian, B. Sethi, and X. Cao, “Sterilization techniques for biodegradable scaffolds in tissue engineering applications,” *J. Tissue Eng.,* vol. 7, May 2016.

4. Methods of Characterization

4.1 Evaluating hydrophobicity

Contact angle measurements (CAMs) are used to obtain information about the hydrophilicity or surface energy of a material. For this project, we want to use CAMs to show the incorporation of soy lecithin changes the hydrophobicity of PCL. A CCD camera (STC-MB202 by Sentech Services) is used to image these angles. The sessile drop method is utilized, and a single droplet of double-distilled deionized water is dropped onto a sample of each of the scaffolds using a pipette. The angle between the liquid-solid interface and liquid-vapor interface is considered the contact angle [1]. Figure 4.1 shows the sessile drop method and how the contact angle is obtained [2]. The angles of each sample are analyzed using an ImageJ plugin DropSnake. All samples with lecithin will show complete wetting and no angle will be captured. Knowing the hydrophilicity of the scaffolds is crucial because we must be able to predict how the material will react in the human body.

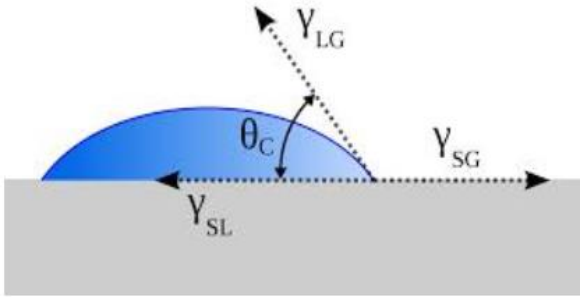

Figure 4.1 [2] The contact angle in the sessile drop technique is the angle between the solid-liquid interface and the liquid-vapor interface

4.2 Analyzing Thermal Properties

4.2.1 Differential Scanning Calorimetry

Differential scanning calorimetry, or DSC, is a thermal analysis technique that can measure thermal transitions. It is imperative that the melting temperature of the blends be well above that of the human body, so premature degradation does not occur. Each DSC has a temperature-controlled furnace that contains a reference pan and a sample pan, demonstrated in Figure 4.2. The furnace is heated at a specific rate, keeping the sample pan and the reference pan at a zero-temperature difference. The reference is used as a control, so it is necessary that it be inert and will not undergo any transitions in the temperature range being measured [1]. When the PCL melts, the endothermic reaction (heat goes into the sample pan) is measured, and a heat flow vs. temperature graph is generated. The transition can be observed where the otherwise linear curve deviates.

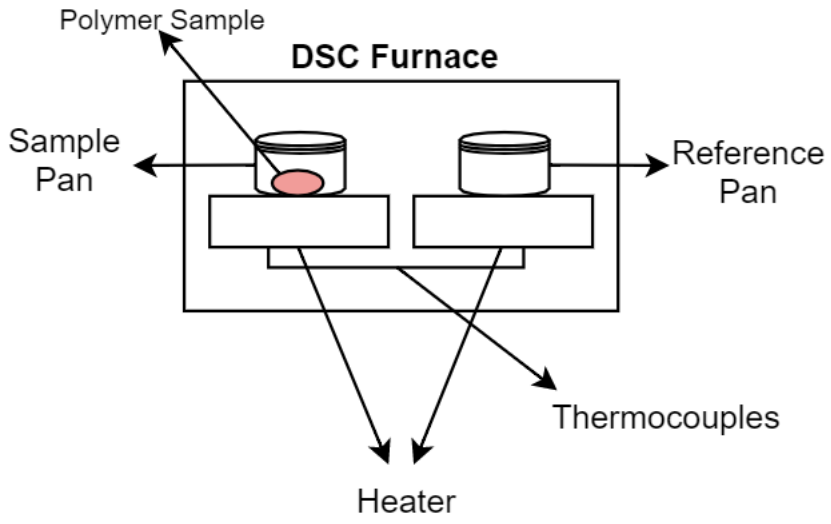

Figure 4.2 Adapted [1] The DSC holds two pans, a sample pan that contains the polymer, and a reference pan that is empty and acts as a control. Each pan has a heater and a power supply. The pans are wired to thermocouples to act as a temperature sensor. The temperature is increased at a steady rate, and changes in heat of the two pans are measured about the change in temperature. When the sample undergoes a change, more heat will flow to the sample than the reference to maintain the same temperature and this difference is measured to form the DSC curves.

For this project, a modulated DSC (Q2000 DSC manufactured by TA Instruments) was utilized to determine the thermal stability of the scaffolds, specifically melt temperature. In preparation, each sample was punched into 4.5 mm circles (n=3). Aluminum pans were weighed, the sample was placed in the pan, sealed and reweighed. One pan was left empty to be used as a reference. The samples were subject to a modulation period of 80 seconds followed by a heating rate of a rate of 5 ºC/min from 5 ºC to 120 ºC. The results of the DSC were then analyzed using the TA Universal Analysis Program.

4.2.2 Thermogravimetric Analysis (TGA)

Thermogravimetric Analysis (TGA) is utilized to explore thermal properties further. TGA measures the weight loss of a material as a function of temperature or time. This technique will predict how stable a material is at high temperatures, and it can also be used to determine the chemical composition. A TGA has a very accurate balance inside of a furnace that uses a null-balance principle. The balance measures changes in the mass of the sample due to degradation or oxygen adsorption [3]. A current is induced to measure the movement of the pans and return them to the original position. The current applied is proportional to mass lost [1].

A Q5000 TGA (TA Instruments) was used to determine the temperature of decomposition of the scaffolds. The samples were placed in 100 µL platinum pans and heated at a rate of 10 ºC/min to a final temperature of 500 ºC. R. Nirmala et al. [4] shows the degradation temperature of lecithin is 160 ºC, and PCL degrades by a two-step weight loss at approximately 250 °C and 350 °C [5]. This data was used to confirm the

degradation and composition of the tested scaffolds. The peaks were analyzed using TA Universal Analysis program.

4.3 Analyzing Chemical Composition

Fourier Transform Infrared spectroscopy, or FTIR, is a characterization technique that gives the chemical composition of a sample. It can be used to show chemical reactions and identify unknown chemical compounds. This technique is used to determine whether the soy lecithin stayed in solution after electrospinning, and to ensure the chemical composition of PCL was not altered while electrospinning. It can also be utilized to ensure the solvents have evaporated and did not remain in the scaffold. An IR spectrum can be measured by scanning a sample with continuous IR wavelengths. Specific wavelength frequencies can be absorbed into specific chemical bonds, which will create a corresponding peak at that wavelength [1].

A Nicolet 6700 FTIR (Thermo Scientific, Waltham, MA) was used for this project. Scans were taken of each sample type at 32 scans with a 4 cm^{-1} resolution with a spectral range of 500-4000 cm^{-1}. It is imperative that the molecular structure of lecithin and PCL be the same before and after electrospinning to ensure their properties remain intact. The peaks for PCL and lecithin are already known based on chemical composition and can be determined from an FTIR chart. PCL and lecithin have similar methyl, carbonyl, and C-O functional groups; however, the peaks indicative of lecithin are higher methyl stretching at 2900 cm^{-1} and the presence of phosphine oxide stretching at 1100 cm^{-1}.

4.4 Fiber Alignment

Scanning Electron Microscopy, or SEM, is most commonly used to obtain a detailed image of the surface or structure of a material on the micro- or nanoscale by raster scanning the surface with an electron beam. In the case of electrospun PCL, it is used to analyze the average fiber diameter and whether there are any defectors or beads on the fiber. It can also be used to identify the presence and location of AuNPs. A limitation of this characterization technique is that the sample must be conductive or sputter-coated with a conductive material [1]. Since PCL is not conductive an environmental SEM (ESEM) can be used.

The samples were imaged on a Quanta 600 FEG Environmental Scanning Microscope at the Electron Microscopy Core Facility. Samples were kept in low vacuum mode and were analyzed at 100X, 1,000X, and 5,000X magnification with a 10kV electron beam. The secondary electron detector was used to form an image of the fibers and the average diameter was analyzed using ImageJ. The backscattered electron detector is utilized to image the AuNPs. Images using backscattered electrons have bright spots where heavier elements are present. BSE signal intensity is proportional to the atomic number of the sample, so heavier elements have higher intensity, presenting as brighter spots [1]. Energy-dispersive X-ray spectroscopy (EDS) was utilized to confirm that bright spots from the BSE micrograph were gold.

4.5 Attachment of Gold

Neutron Activation Analysis (NAA) is used to quantify the presence of an element, in this case gold. To perform this technique, the sample is bombarded with

neutrons creating radioisotopes. As the isotopes decay, a beta particle and delayed gamma rays are emitted. A schematic of this progression can be seen in Figure 4.3. The emitted gamma rays are used to determine which elements are present in the sample and the number of gamma rays with a specific energy will quantify that element [9]**.** When a sample containing gold is irradiated, the ^{197}Au absorbs a neutron and becomes ^{198}Au, so the reaction is ^{197}Au + n → ^{198}Au. It is also known that ^{198}Au is a β emitter, so when the ^{198}Au decays to ^{198}Hg, a 411.8 keV gamma ray is emitted 95.62% of the time (^{198}Au → β^- + ^{198}Hg + γ (411.8 keV)) [10]. The amount of gold in the original sample is quantified by counting the number of 411.8 keV rays emitted from the sample after the sample has been exposed to neutrons. This technique is called standard comparator instrumental NAA.

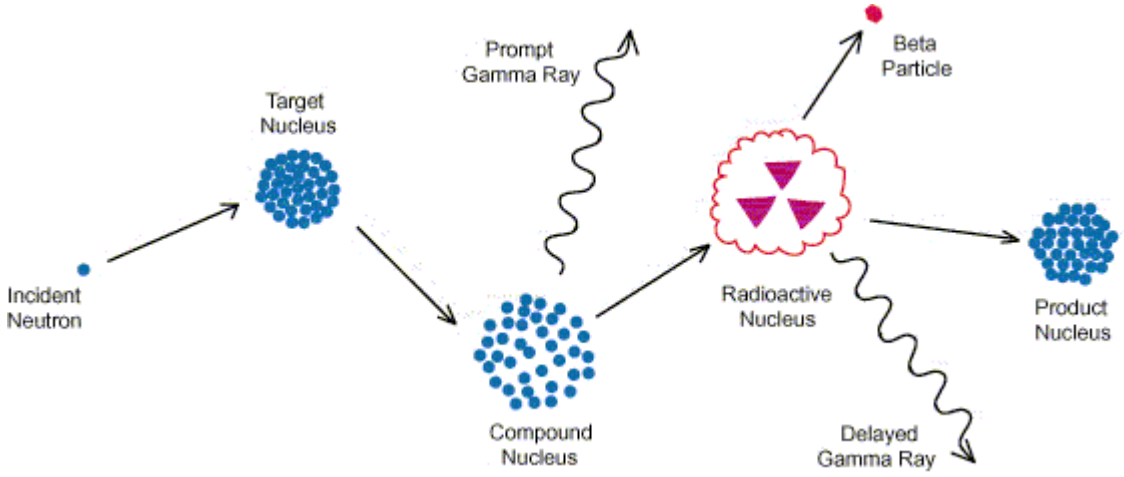

Figure 4.3 [9] Neutrons bombard the surface of a sample to create radioisotopes, in turn emitting delayed gamma rays. These gamma rays are used to determine and quantify each element found in the material.

Samples are punched, lyophilized and weighed as preparation. They are placed in high-density polyethylene NAA vials where they are taken to the University of Missouri Research Reactor Center for analysis. The samples were loaded into two rabbits and irradiated for 2 minutes. Samples decayed for up to 7 hours before being counted with an

automated sample changer and Canberra High Purity Germanium (HPGe) detector. Once the data was collected, Canberra-VMS Genie 2000 software was used for gamma-ray peak fitting, and Au concentrations were recorded in Microsoft Excel.

4.6 Characterizing Scaffold Biocompatibility

4.6.1 Cell Culture Protocol

All cell studies in this project were performed with L929 murine fibroblast cells. A reliable protocol is used to pass, count, and store the cells. The cells used for assays are passed weekly. For each passage a 1:12 (cell suspension: cell media) flask is used. The media in the flask is removed, and the flask was rinsed with 5 mL of Dulbecco's phosphate buffered saline (DPBS). 1 mL 0.25% trypsin-EDTA is placed in the flask and incubated for 1 to 2 minutes to detach the cells from the bottom of the flask. Before continuing, the flask should be examined under a microscope to ensure the cells are rounded and floating freely. 10 mL of warmed sterile cell media is added to the cell culture flask then transferred to a 15 mL centrifuge tube. The solution was spun down in a Z200A centrifuge (Hermle, Wehingen, DE) at 1,250 rpm for 7 minutes. While the solution is in the centrifuge, the new flasks are labeled, and 5.5 mL of cell culture media is added. When the centrifuge stops, the tube is taken back to the biological hood, and without disturbing the pellet, 9 mL of the liquid is pipetted into the waste beaker. 4 mL of fresh cell media is then added to the tube with cells and resuspended. If an assay is being performed, the cells are counted at this time. For weekly subculturing, a 1:12 flask and 1:144 flask is prepared and placed in the incubator at 37 ºC and 5% CO_2 until needed.

4.6.2 WST-1 Cytotoxicity Assay

Cell studies should be used to look at cytoxicigty of the scaffolds created to detect cell viability once cells and scaffolds are integrated together. Cell viability can be found using a water-soluble tetrazolium (WST) assay. WST-1 is a tetrazolium salt that is cleaved to a formazan dye by cellular enzymes [11]. This assay is advantageous to similar assays because the final reagent is water-soluble, so it requires fewer steps. An increase in the number of live cells causes an increase in enzyme activity, which leads to an increase in the amount of formazan dye formed. The amount of formazan dye that is formed is directly related to the number of active cells in the assay. The formazan dye can be quantified using a spectrophotometer measuring absorbances at 655 nm and 450 nm and subtracting the two. This assay is often performed in 3, 7, and 10-day time-points.

For this project, a 3-day assay was performed. To prepare, n=6 of each sterilized scaffold type (PCL, 40:40, 50:50, and 50:50 with10% AuNP) was placed in a 96-well

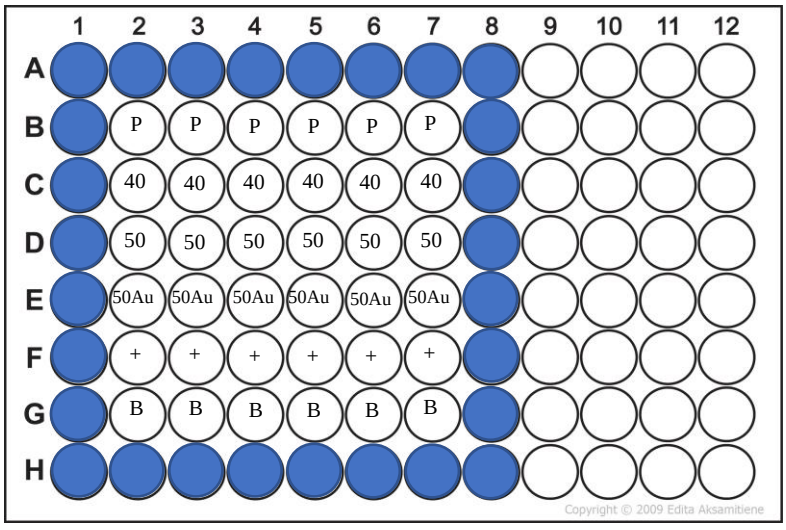

Figure 4.4 [12] Plate map for the WST-1 Assay. P corresponds to PCL, 40 corresponds to 40:40, 50 corresponds to 50:50, 50 Au corresponds to 50:50 with 10% AuNP, + corresponds to a positive control of only cells, and B corresponds to a blank of only cell media.

plate, as indicated on the plate map (Figure 4.4). 150 μL of supplemented cell media (EMEM + 10% (v/v) horse serum + Penn Strep (200 U/mL)) is added to each well containing a sample. PBS is placed in the outer wells to prevent the evaporation of the cell media. The well plate is then incubated at 37 ºC and 5% CO_2 for 24 hours.

After the incubation period, the cells are prepared, counted, and placed in the microplate to be incubated for 72 hours. The cells will go into each well with a sample, as well as an additional row with only cells to be used a positive control. Cell culture media will be placed in a row by itself to be used as a blank. This assay was performed with L929 murine fibroblast cells at a concentration of 0.75×10^4 cells/mL.

After the 72-hour incubation period, the cell media is removed from the well-plate, and 25 μL of WST-1 reagent is added to each well. WST-1 is light sensitive, so the lights must be turned off when the reagent is exposed. Once added, the plate is incubated for 4 hours, where the WST-1 is cleaved to formazan dye. 100 μL of the media is taken from each well and placed in a separate 96-well microplate, and a Biotek Cytation 5 cell imaging Multi-Mode plate reader is used to obtain an absorbance measurement, read at 450 nm with a 650 nm reference.

4.6.3 Reactive Oxygen Species Assay

Accumulation of reactive oxygen species (ROS) is known to cause damage to biomolecules in the body. Specifically, for this project, too much ROS will result in unwanted inflammation [12]. This assay uses 2',7'-Dichlorodihydrofluorescein diacetate (DCFH-DA), which is cell-permeable. This DCFH-DA diffused into the cells and is broken down by cellular esterase activity to DCFH. When ROS is present, DCFH is then

oxidized to fluorescent DCF. Fluorescence intensity is directly related to ROS levels. Therefore the ROS produced can be quantified against the fluorescence of a known DCF standard [13].

To perform this assay, 0.25 mL of cell suspension is placed in the corresponding wells of a 96-well plate with a cell concentration of 4.42 x 10^4 cells/mL. The cells are then incubated for 24 hours. DCFH-DA is diluted to 1X in DPBS and added to the cells in each well before incubating for one hour. Sterilized samples (n=6) of PCL, 1% with lecithin, 5% with lecithin, and 10% with lecithin are added to the corresponding wells as well as a negative control of only cells, and a positive control of 50 mM hydrogen peroxide. The plate was allowed a 12-hour incubation period where the DCFH-DA is cleaved to DCF. The plate map for this study can be seen in Figure 4.5. The assay is terminated with 2X cell lysis buffer and 0.1 mL of the solution is transferred to a separate 96-well plate to be read. A standard curve is prepared with a 1:10 series dilution of DCF standards with a concentration range from 0-10 μM and placed in the second 96-well

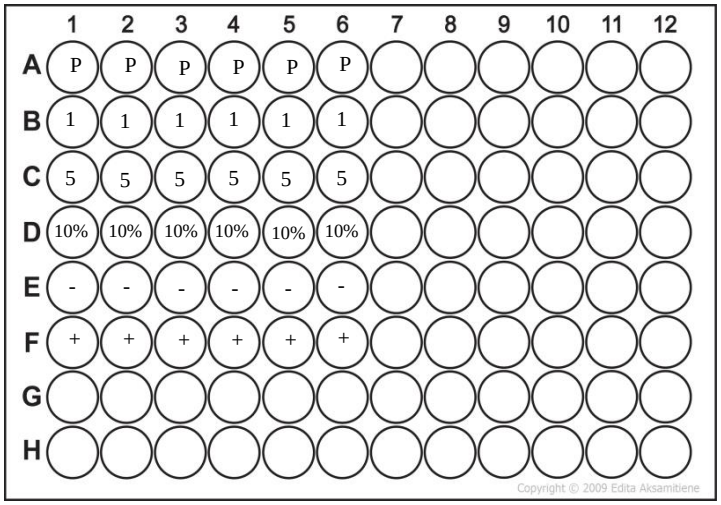

Figure 4.5 [12] Plate map for the ROS Assay. P corresponds to PCL,1% corresponds to 1% with lecithin, 5% corresponds to 5% with lecithin, 10% corresponds to 10% with lecithin, - corresponds to a negative control of only cells, and + corresponds to a positive control with 50 mM hydrogen peroxide.

plate. Using the Cytation 5 reader, the fluorescence of the second 96-well plate is read at 530 nm emission and 480 nm excitation.

4.7 Statistical Analysis

The results of the experiments were analyzed using OriginLab. A one-way analysis of variance (ANOVA) with Tukey-Kramer post-hoc tests were performed to determine the statistical significance ($p < 0.5$) of the results.

4.9 References

[1] S. Zhang, L. Li, and A. Kumar, *Materials Characterization Techniques*, 1st ed. Taylor & Francis Group, 2009.

[2] J. Gillis, *Contact angle*. 2006.

[3] M. McKinnon, "Thermogravimetric Analysis (TGA) & Differential Scanning Calorimetry (DSC)."

[4] R. Nirmala, K. T. Nam, D. K. Park, B. Woo-il, R. Navamathavan, and H. Y. Kim, "Structural, thermal, mechanical and bioactivity evaluation of silver-loaded bovine bone hydroxyapatite grafted poly(ε-caprolactone) nanofibers via electrospinning," *Surf. Coat. Technol.*, vol. 205, no. 1, pp. 174–181, Sep. 2010.

[5] R. Nirmala, H.-M. Park, R. Navamathavan, H.-S. Kang, M. H. El-Newehy, and H. Y. Kim, "Lecithin blended polyamide-6 high aspect ratio nanofiber scaffolds via electrospinning for human osteoblast cell culture," *Mater. Sci. Eng. C*, vol. 31, no. 2, pp. 486–493, Mar. 2011.

[6] J. R. Davis, *Tensile testing*. ASM international, 2004.

[7] MCEN 4027: Mechanical Engineering Laboratory, "Experimental Technique - Instron 1," *Mechanical Engineering: University of Colorado Boulder*. [Online]. Available: https://www.colorado.edu/MCEN/MCEN4027/. [Accessed: 16-Oct-2017].

[8] R. L. Mauck *et al.*, "Engineering on the Straight and Narrow: The Mechanics of Nanofibrous Assemblies for Fiber-Reinforced Tissue Regeneration," *Tissue Eng. Part B Rev.*, vol. 15, no. 2, pp. 171–193, Jun. 2009.

[9] "MU Research Reactor - Products and Services - Analytical Services - NAA - Analytical Signal." [Online]. Available: http://www.murr.missouri.edu/ps/ps_analytical_NAA_analytical.php. [Accessed: 12-Apr-2018].

[10] S. P. me, F. Hardeman, P. Robouch, N. Etxebarria, and G. Arana, "NEUTRON ACTIVATION ANALYSIS WITH Ko-STANDARDISATION : GENERAL FORMALISM AND PROCEDURE," p. 110.

[11] H. Tominaga *et al.*, "A water-soluble tetrazolium salt useful for colorimetric cell viability assay," *Anal. Commun.*, vol. 36, no. 2, pp. 47–50, Jan. 1999.

[12] E. Aksamitiene, *96-well pate*. 2012.

[13] R. Spooner and Ö. Yilmaz, “The Role of Reactive-Oxygen-Species in Microbial Persistence and Inflammation,” *Int. J. Mol. Sci.*, vol. 12, no. 1, pp. 334–352, Jan. 2011.

[14] D. A. Bass, J. W. Parce, L. R. Dechatelet, P. Szejda, M. C. Seeds, and M. Thomas, “Flow cytometric studies of oxidative product formation by neutrophils: a graded response to membrane stimulation,” *J. Immunol. Baltim. Md 1950*, vol. 130, no. 4, pp. 1910–1917, Apr. 1983.

5. Results and Discussion

5.1 Evaluation of Contact Angle Measurements

Contact angles approaching 90º indicate a hydrophobic surface. The contact angle of pristine PCL was found to be 96.93º (n=2). The contact angle tests for the 40:40, 50:50 and the Au samples with lecithin all resulted in a 0º contact angle. Several attempts were made using different locations of the sample, and there was complete wettability each time. The wetting shows that the addition of lecithin to the PCL solution makes the scaffold hydrophilic. 0° contact angle measurements, along with surface roughness, have been shown to give a favorable environment for chondrocytes to keep their shape and function correctly [1]. The droplet from hydrophobic PCL and the wetted surface of a hydrophilic blend can be found in the Appendix.

5.2 Thermal Transition Information

5.2.1 Differential Scanning Calorimetry

Heat is required to break down the ordered structure of the solid state to become disordered in the liquid state, meaning this undergoes an endothermic reaction. DSC thermograms (shown in Appendix) plot heat flow vs. temperature and are used to determine thermal transitions. When a sample undergoes a phase change, there is a deviation from linearity of heat flow to temperature. The pans in this study were heated from 5 ºC to 120 ºC at a rate of rate of 5 ºC/min. TA Instrument Analysis software was used to determine the scaffold melting temperatures. The changes in

melting temperatures between the experimental groups are statistically insignificant (shown in Figure 5.1). Lecithin does not show any melting peaks because of its amorphous nature, indicating that the incorporation of lecithin and AuNPs does not alter the thermal transition. The average melting temperature for all samples types was 53.73 ± 0.717 ºC. A melting point of 53 ºC is well above that of the body (37 °C), so it is appropriate for use *in vivo*.

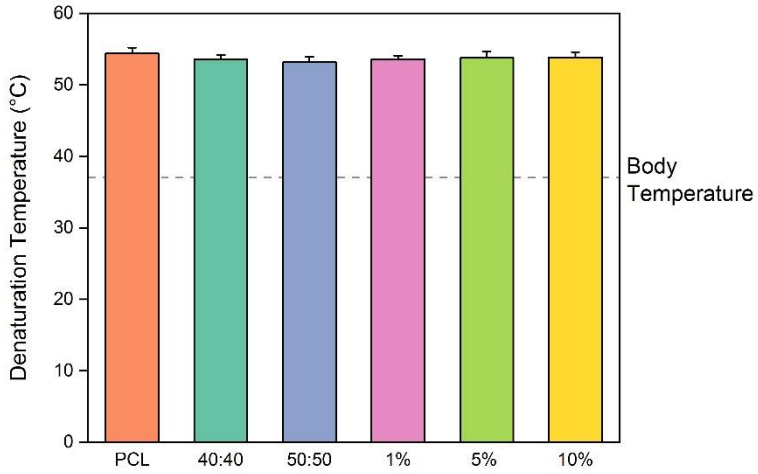

Figure 5.1 DSC analysis results show the average denaturation temperatures with standard deviation error bars. There is no statistical difference between any experimental group. 1% ,5%, and 10% groups contain lecithin.

5.2.2 Thermogravimetric Analysis

The decomposition temperatures were measured using TGA. The samples were heated at a rate of 10 ºC/min to a final temperature of 500 ºC in air. There are two weight-loss peaks for pristine PCL and a slight convexity for lecithin in the blended samples around 160 ºC; this can be seen in the TGA thermograms in Figure 5.2. The degradation temperature for the 50:50 (297.0 ºC ± 7.201) sample was significantly higher than PCL (280.75 ± 0.590) and 40:40 (282.45 ºC ± 3.897) suggesting that the higher concentration of lecithin can improve the thermal stability. This improvement;

however, contradicts the findings of Nirmala et al. where the onset temperatures decreased with the increase in lecithin concentration [2]. There is a possibility that the higher concentration of lecithin is altering the semi-crystalline structure of PCL and will need to be investigated further.

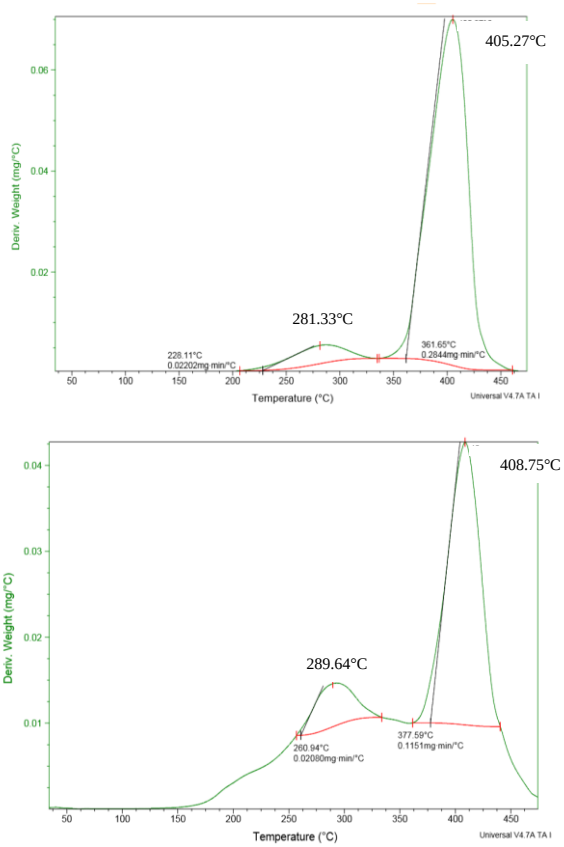

Figure 5.2 TGA thermograms of PCL (top) and 50:50 (bottom). The convexity around 200ºC in the 50:50 sample shows the degradation of lecithin, confirming its presence. The degradation temperature of PCL is also higher in the 50:50 sample, indicating the presence of lecithin improves this characteristic.

5.3 Chemical Composition Analysis

FTIR was utilized to determine further if lecithin was successfully incorporated into the scaffolds. The output of FTIR plots the percent absorbance versus the frequency of infrared radiation. When the chemical bonds absorb the radiation at their resonant frequencies, the absorbance through the sample drastically increases,

resulting in peak formation. FTIR peaks will give the chemical composition of the scaffold. Figure 5.3 shows the peaks of pristine PCL, liquid lecithin, 40:40, and 50:50. Both PCL and lecithin have almost identical peaks at approximately 1720 cm^{-1} and 1160 cm^{-1}, which correspond to carbonyl stretching and C-O stretching respectively. From the spectra, one can see that the peak at 2900 cm^{-1} is stretched more in lecithin and blended samples, this wavelength corresponds to methyl stretching (hydrocarbon bonds). Because lecithin is a fatty acid, integration of lecithin into the scaffolds would show an increase in methyl stretching and methyl groups. Additionally, lecithin has a phosphine oxide (P=O) functional group not present in PCL. This phosphine oxide stretching can be found at1100 cm^{-1} on the lecithin blends, but not observed on the pristine PCL as expected. The presence of the phosphine peak, as well as the increase in methyl stretching, indicates that lecithin

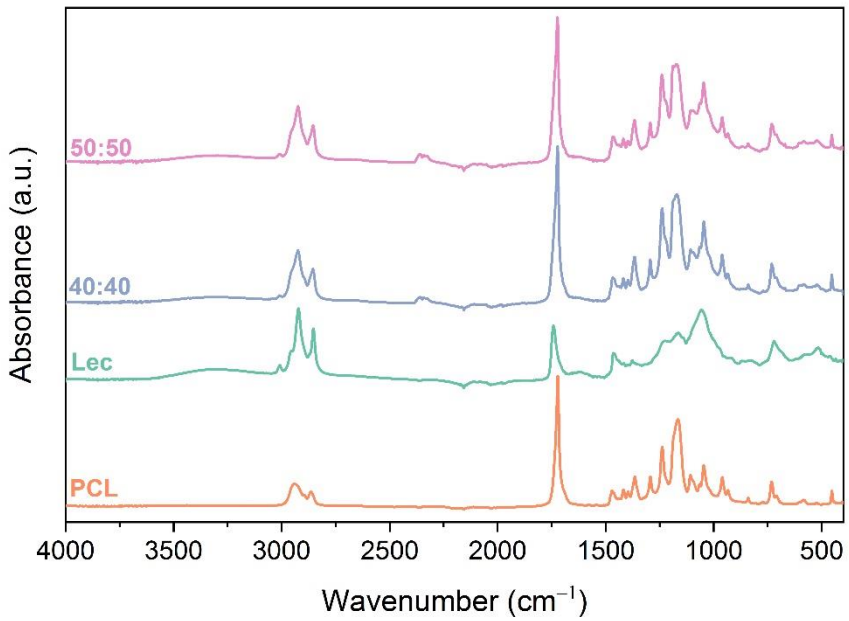

Figure 5.3 FTIR spectra of electrospun PCL, liquid lecithin, 40:40, 50:50, and is observed. PCL exhibits three prominent peaks which correspond to hydrocarbon bonds and give rise to the presence of an ester group. Lecithin has a higher peak for methyl stretching, as well as an additional peak for its phosphine oxide functional group.

was successfully incorporated into the scaffolds. Chloroform has very prominent peaks at 800 cm^{-1} and 3000 cm^{-1}, so it is evident that it is not present in the scaffolds. DMF however, has very similar peaks as PCL, so the scaffolds should undergo lyophilization to dry out any remaining solvent [3].

5.4 Fiber Alignment and Orientation

To determine fiber alignment of each scaffold, as well as observe the presence of AuNPs where appropriate, scanning electron microscopy was performed. Each SEM image has a scale bar showing the magnification the image was taken, allowing the properties of the scaffold to be analyzed with the ImageJ. Upon visual inspection of the micrographs, the PCL (Figure 5.4 left) has unforeseen pores on the fiber. This sample was fabricated in the summer, where the humidity in the room was very high, the condensation can create porous structures. It is unknown whether these pores are beneficial to this study at the time, but they will be further investigated.

The 40:40 sample (Figure 5.4 right) appears to have the most desirable formation, with elongated strands and no beading. This fiber orientation is ideal because it mimics the extracellular matrix and will be able to support cellular activity, the fiber diameters for all sample types can be seen in Table 5.1. SEM images were necessary because the scaffolds all look the same to the naked eye, but after seeing the detailed surfaces, it is apparent that changes need to be made during the electrospinning process. Most of the samples shown in the Appendix would not be an appropriate scaffold for tissue engineering because the fibers are not polymerized, and the porosity no longer mimics the ECM.

Table 5.1 The average fiber diameter for both nano- and micro- fibers can be seen for PCL, 40:40, 50:50, and 50:50 10% AuNP.

	Fiber Diameter	
	Nanofibers (nm)	*Microfibers (μm)*
PCL	367 ± 109	2.16 ± 0.81
40:40	429 ± 107	3.64 ± 0.60
50:50	406 ± 82	2.78 ± 0.08
50:50 + 10% AuNP	800 ± 156	3.64 ± 1.2

Images taken with the backscattered electron detector have bright spots where the AuNPs are located, a 50:50 10% AuNP scaffold at 1,000X magnification is shown in Figure 5.5 along with its EDS analysis. The EDS spectra confirmed the presence of gold as well as aluminum and salt. Aluminum fragments remain since the fibers were collected on foil when electrospun. There are other elements on the surface because these have been exposed to many surroundings and have not been sterilized. All of the SEM micrographs can be found in the Appendix.

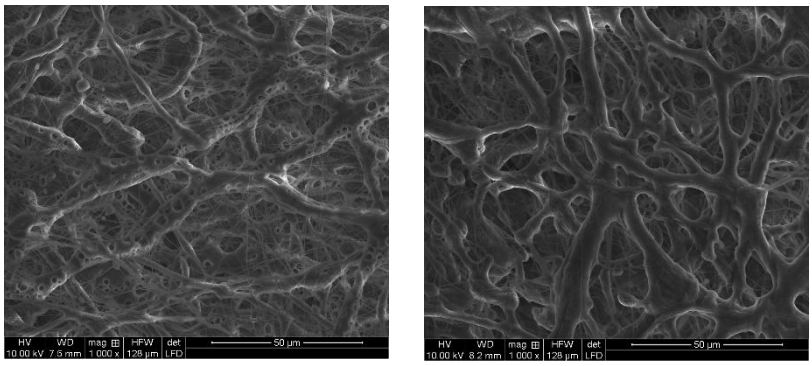

Figure 5.4 SEM images of electrospun scaffolds shows the nonwoven fiber morphology of the samples at 1000X magnification and 10 kV; (left) PCL, (right) 40:40. The PCL has pores on the fibers from the humid environment it was electrospun. These were unexpected, but potentially beneficial. The 40:40 sample shows appropriate fiber formation with no defects.

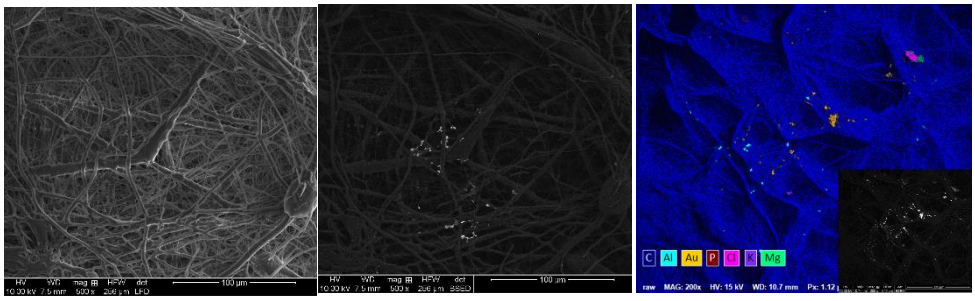

Figure 5.5 SEM images of 50:50 10% AuNP at 1000X magnification. (Left) Secondary electron detector gives images that show the fiber alignment, (middle) the backscattered electron detector highlights heavier elements with bright spots, (right) EDS performs elemental analysis confirming the presence of Au. Al is present due to the foil backing of the scaffolds, other elements are present because the samples have not been sterilized and they have been exposed to a lab environmenet.

5.5 Gold Nanoparticle Integration

The neutron activation analysis (NAA) results offer a quantitative analysis of AuNP. As expected, the number of nanoparticles present increased with the volume incorporated into the electrospun solution: 1% (1.075 ± 0.068), 5% (6.81 ± 0.243), and 10% (9.2 ± 1.058). Figure 5.6 shows the number of nanoparticles before sterilization for scaffolds containing lecithin. NAA was performed first on non-sterile samples, and then on sterile samples to confirm the nanoparticles are incorporated

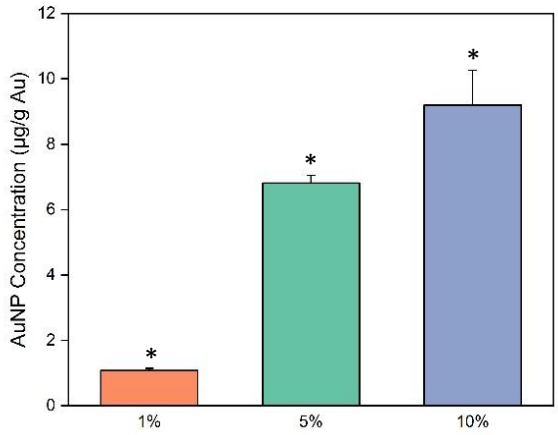

Figure 5.6 Results of Neutron Activation Analysis show as the concentration of 20 nm AuNP increases in solution, it also increases in scaffold.

into the bulk of the scaffold and not washed away on the surface. When normalized, the contents do not come out to be exactly 1%, 5%, and 10% of each other, but they follow this trend rather closely. This experiment confirms that altering the concentration of AuNP in solution alters the concentration of AuNP in the electrospun scaffolds.

5.6 Biocompatibility Response

5.6.1 WST-1 Assay

The WST-1 Assay was performed using L929 fibroblast cells to measure cell viability. This assay used a 3-day time point, but future studies should use a 7 - and 10 - day assay to ensure there are no discrepancies in the data. Although the 50:50 samples were significantly different from the PCL, all of the samples used have appropriate margins of cell viability (Figure 5.7). These results show that the incorporation of lecithin does not create a cytotoxic environment for the fibroblast

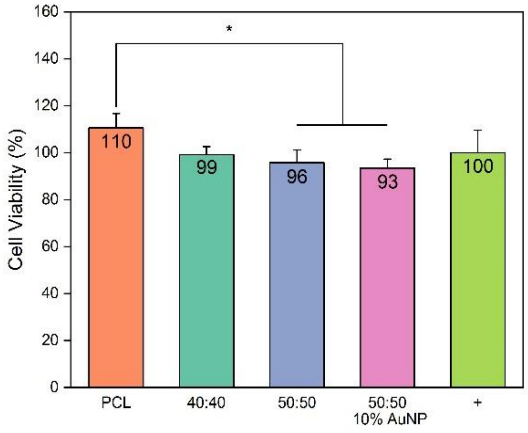

Figure 5.7 WST-1 Results for a three-day time point. % Cell viability was normalized to a positive control, showing that even though 50:50 and 50:50 10% AuNP were significantly different from PCL, all sample types showed low cytotoxicity.

cells. Fibroblast cells were used as a baseline study, in the future chondrocytes should also be used for these assays since they are the natural healing cells in articular cartilage. The 50:50 10% AuNP results also show that the nanoparticles have good cell viability, which is consistent with literature findings [3]. Literature has also demonstrated that nanoparticle size can drastically affect cell cytotoxicity. Small particles (< 2 nm) are endocytosed into cells and lead to cell death. AuNPs with a diameter >5 nm have biologically inert properties, but if the size is too large, it will not affect cytotoxicity[3]. Because the nanoparticles were not modified, and they are relatively large, and low cytotoxicity was expected.

5.6.2 Reactive Oxygen Species Assays

Reactive oxygen species (ROS) are an inevitable byproduct of oxygen metabolism, but antioxidants keep this production in check to minimize the damage to biomolecules. In the past, ROS was thought to have only harmful effects, but studies have shown that low concentrations can be attributed to regulating cell signaling cascades for wound healing and fostering angiogenesis [4]. As long as the antioxidants are keeping the ROS levels under control, ROS assists in chondrocyte activation and proliferation; regulating cartilage homeostasis [5]. Elevated levels of ROS on the other hand, cause oxidative stress to the tissue resulting in structural and functional cartilage damage [5].

An ROS assay was performed using L929 Fibroblast cells to measure the free radical scavenging that occurs on the mats. This assay uses fluorescent intensity to quantify the ROS present. A standard curve ($r^2 = 0.996$) was created using DCF

standards from 0.001 to 10,000 nM concentrations. A 50 mM Hydrogen Peroxide positive control was used; however, this concentration was too high, which possibly killed all of the cells, and did not result in significantly high ROS production as it should have. Figure 5.8 shows that the 1% **(**120.211 ± 30.004**)** concentration of gold and the 10% (90.369 ± 18.202) concentration were significantly larger. Moving forward the 5% (53.737 ± 17.903) will be investigated further as well as 100 nm AuNPs. This ROS generation could be attributed to the presence of lecithin, so more assays should be conducted to rule this out.

Previous research has implied that scaffolds with higher AuNP concentrations produce more ROS. However, it was thought that free radical generation could be dependent on size rather than concentration. The results of this study showed that 100 nm AuNP groups with varying concentrations did not produce too much ROS, and different concentrations with 20 nm AuNP generated free radicals [6]. Based on these findings, 100 nm AuNPs should be investigated with 20 nm AuNPs.

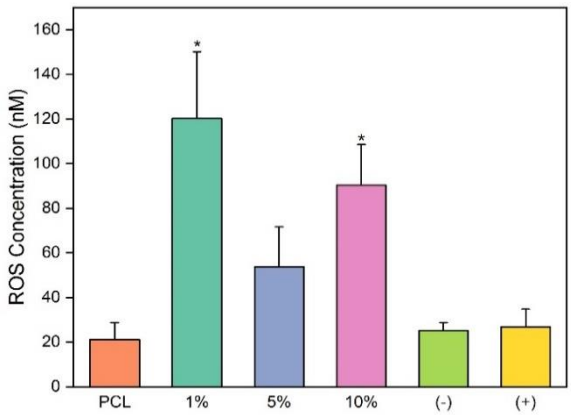

Figure 5.8 ROS Concentration is determined from a DCF standard curve. ROS concentration of 1% and 10% AuNP with lecithin were significantly higher than PCL. The positive control was made form 50 mM hydrogen peroxide at too high of a concentration to produce a significant amount of ROS because the cells were most likely dead.

5.9 References

[1] W. Janvikul, P. Uppanan, B. Thavornyutikarn, W. Kosorn, and P. Kaewkong, "Effects of Surface Topography, Hydrophilicity and Chemistry of Surface-treated PCL Scaffolds on Chondrocyte Infiltration and ECM Production," *Procedia Eng.*, vol. 59, pp. 158–165, Jan. 2013.

[2] R. Nirmala, H.-M. Park, R. Navamathavan, H.-S. Kang, M. H. El-Newehy, and H. Y. Kim, "Lecithin blended polyamide-6 high aspect ratio nanofiber scaffolds via electrospinning for human osteoblast cell culture," *Mater. Sci. Eng. C*, vol. 31, no. 2, pp. 486–493, Mar. 2011.

[3] "Formamide, N,N-dimethyl-." [Online]. Available: https://webbook.nist.gov/cgi/inchi?ID=C68122&Type=IR-SPEC&Index=2. [Accessed: 25-Apr-2018].

[4] Z. Liu *et al.*, "Effects of Internalized Gold Nanoparticles with Respect to Cytotoxicity and Invasion Activity in Lung Cancer Cells," *PLOS ONE*, vol. 9, no. 6, p. e99175, Jun. 2014.

[5] S. Di Meo, T. T. Reed, P. Venditti, and V. M. Victor, "Harmful and Beneficial Role of ROS," *Oxid. Med. Cell. Longev.*, 2016.

[6] Y. Henrotin, B. Kurz, and T. Aigner, "Oxygen and reactive oxygen species in cartilage degradation: friends or foes?," *Osteoarthritis Cartilage*, vol. 13, no. 8, pp. 643–654, Aug. 2005.

[7] Cozad Matthew J., Bachman Sharon L., and Grant Sheila A., "Assessment of decellularized porcine diaphragm conjugated with gold nanomaterials as a tissue scaffold for wound healing," *J. Biomed. Mater. Res. A*, vol. 99A, no. 3, pp. 426–434, Sep. 2011.

6. Conclusions

6.1 Review of Research Objectives

Osteoarthritis (OA) is a crippling condition that millions of people suffer from because articular cartilage is unable to regenerate. This reinforcing material will prolong the stability of the knee joint, delaying the need for very invasive surgery. The aim of this project was to electrospin a hybrid polymer scaffold that is biocompatible and nontoxic, that can withstand the natural environment of the knee. The hybrid blends consisted of PCL, lecithin, and 20 nm gold nanoparticles in varying concentrations. The polymer blends consisted of 40% (wt/v) solute:40% (wt/wt) lecithin and 50% (wt/v) solute:50% (wt/v) lecithin. 1% (v/v), 5% (v/v), and 10% (v/v) AuNP concentrations were also investigated with fixed amounts of lecithin and PCL. All of these scaffolds were compared to pristine PCL as a control group. It was hypothesized that if the properties of each component were optimized, a superior scaffold for potential use as a cartilage protectant could be fabricated. Three primary objectives were examined:

Objective 1: Optimize electrospinning parameters to achieve homogeneous mats with varying concentrations of PCL, soy lecithin, and 20 nm gold nanoparticles

- This objective was reached; however, electrospinning is so sensitive to environmental factors that reproducibility is difficult. SEM images also showed that some of the scaffolds with more lecithin did not have complete polymerization, the flow rate when using 50% lecithin should be slowed to

correct this. It has also been discovered that DMF dissolves the tubing used, which could affect the scaffold production. Future scaffolds should be fabricated with different tubing.

Objective 2: Characterize each scaffold to determine which solution ratio is best for attachment. Bulk and surface characteristics will be examined with pristine PCL as a control.

- Contact angle measurements determined hydrophilicity; Fourier Transform Infrared Spectroscopy gave chemical characteristics; Differential scanning calorimetry (DSC) and Thermogravimetric analysis (TGA) were conducted to evaluate thermal properties of the scaffolds; Scanning electron microscopy (SEM) was utilized to observe the fiber alignment and defects, as well as the presence of AuNPs; Neutron Activation Analysis quantified the nanoparticles in each scaffold.

Objective 3: Characterize biocompatibility and cytotoxicity of scaffolds

- A WST-1 assay was employed to show that the samples were non-toxic.
- A reactive oxygen species (ROS) assay was performed to establish the biocompatibility of the scaffolds.

6.3 Conclusions from Characterization

6.3.1 Stability of Scaffolds

The hydrophobic properties were tested by taking contact angle measurements. The blended scaffolds had complete wettability, showing lecithin creates a hydrophilic surface to foster a healthy environment.

The thermal melting temperatures of the scaffolds were determined using DSC. There were no significant differences between any of the sample types. The average melting temperature of all experimental groups was 53.73 ± 0.717 ºC. Thermogravimetric analysis gave the degradation temperature of the scaffolds. 50:50 (297.0 ºC ± 7.201) was significantly higher than 40:40 (282.45 ºC ± 3.897) and PCL (280.75 ± 0.590), showing excellent thermal stability that can withstand physiological temperatures.

FTIR was conducted to ensure lecithin was still part of the bulk material after electrospinning and PCL maintained its chemical composition. The spectra showed PCL has prominent peaks at 2900 cm^{-1}, 1720 cm^{-1} and 1160^{-1} which correspond to methyl stretching (hydrocarbon bonds), carbonyl stretching (C=O), and C-O stretching. Lecithin shares the same peaks as PCL; only it will have a higher methyl peak from its multiple hydrocarbon chains. It will also have an additional peak for the presence of a phosphine group at 1100 cm^{-1}. The samples should undergo lyophilization to ensure all of the solvents have been removed after electrospinning.

6.3.2 Attachment of Gold

SEM analysis verified the presence of AuNPs with the secondary electron detector. SEM images also showed the fiber alignment. Visually each concentration gave rise to randomly oriented nanofibers mimicking the natural extracellular matrix; each scaffold had nano- and microfiber formation.

To quantify the nanoparticle concentration, NAA was performed. This experiment concluded that scaffolds with a higher concentration of AuNPs mixed in solution have a higher number of AuNPs attached to the scaffold after electrospinning. 4.5 mm punches were used (n=3) and it was determined that 1% had 1.075 ± 0.068 AuNPs, 5% had 6.81 ± 0.243 AuNPs, and 10% had 9.2 ± 1.058 AuNPs. NAA was also conducted after sterilization to ensure the nanoparticles were not washed away, giving rise to the same trend as before sterilization. Sterilization would need to be conducted before any implantation of a scaffold, so this is vital information.

6.3.3 Biocompatibility of Scaffolds

A WST-1 assay confirmed that all sample types have low cytotoxicity. When normalized to the positive control, 50:50 and 50:50 10% AuNP are significantly different from PCL but still have 96% and 93% cell viability respectively, indicating that cells were able to survive in the presence of each sample.

An ROS assay was conducted to assess the biocompatibility with varying gold concentrations. The 1% (120.211 ± 30.004) and the 10% (90.369 ± 18.202) AuNP concentrations produced significantly more ROS than PCL and 5% (53.737 ± 17.903). These results indicate that 5% (v/v) AuNP is the optimal concentration to lower

inflammatory response. The ROS generation could be attributed to the presence of lecithin, so another assay should be conducted with the 40:40 and 50:50 samples.

6.4 Proposed Future Investigations

The superficial zone of the articular cartilage protects the deeper layers, and the proposed scaffold should mimic this. This layer has tightly aligned collagen fibrils running parallel to the articular surface. This layer is responsible for most of the tensile properties, allowing it to withstand tensile, shear, and compressive forces on the joint [1].

The PCL/lecithin/AuNP scaffolds need to undergo tensile testing to quantify Young's modulus (resistance to deformation), maximum strain, and stress at failure. This test is performed to determine if the incorporation of lecithin or AuNPs will strengthen the tensile properties. Compression tests and shear/friction tests must also be conducted to ensure the samples will not tear or break down in the harsh dynamic environment of the knee. Previous research has shown that the addition of lecithin to the scaffolds weakens the stability slightly, but this is to be compared to natural tissue to understand the deficit [2].

Based on the findings of this work, 40:40 scaffolds with 5% 20 nm AuNPs should be fabricated and undergo cell studies and mechanical testing. Based off of the work done by Cozad[2], 40:40 scaffolds with 100 nm AuNPs should also be electrospun and cell studies compared with PCL and 40:40 as a control. The electrospinning parameters might need adjustment with the introduction of different sized nanoparticles.

Chondrocyte cells are responsible for the production of the cartilage ECM, which would make them a logical choice to be used in a cartilage study [3]. Chondrocyte cells are more sensitive than fibroblast cells, so to ensure biocompatibility and low cytotoxicity in the environment of the knee, WST and ROS assays should be conducted with this cell type.

The primary application for this scaffold is to act as a reinforcing material, but for it to foster any regrowth, cells must be able to infiltrate the surface. To see if cells can infiltrate the scaffold a PicoGreen assay can be conducted. The reagent used is a sensitive fluorescent dye that quantifies double-stranded deoxyribonucleic acid (dsDNA). The reagent incubates and binds with dsDNA that is present in cells that have infiltrated the scaffolds [4].

Studies have shown that where inflammation occurs, a higher number of macrophages are present. It has even been looked at to target macrophage activation as a potential OA treatment [6]. A macrophage inflammatory Assay could be performed to determine if the scaffolds induce anti-inflammatory macrophages. The macrophage cell line would be suspended with lipopolysaccharide (LPS) and seeded in a well-plate with the scaffolds. The medium is placed in a new plate, and a cytokine profile is created, where the pro-inflammatory cytokines (TNF-α) and anti-inflammatory cytokine (interleukin-10) are measured [7].

Studies should be conducted on animal joints to evaluate different attachment methods in a dynamic environment. Large animal models that are appropriate for osteoarthritis studies are canine, sheep or horse, however, the horse AC is the closest animal model to humans [5]. The fixation methods looked at should include fibrin glue

attachment, suturing, and subchondral anchoring, based on the study performed by Drobnic et al. [6]. Once the attachment method has been determined, *in vivo* studies with the scaffold should be conducted.

6.5 References

[1] A. J. Sophia Fox, A. Bedi, and S. A. Rodeo, "The Basic Science of Articular Cartilage," *Sports Health*, vol. 1, no. 6, pp. 461–468, Nov. 2009.

[2] M. Zhang, K. Wang, Z. Wang, B. Xing, Q. Zhao, and D. Kong, "Small-diameter tissue engineered vascular graft made of electrospun PCL/lecithin blend," *J. Mater. Sci. Mater. Med.*, vol. 23, no. 11, pp. 2639–2648, Nov. 2012.

[3] Cozad Matthew J., Bachman Sharon L., and Grant Sheila A., "Assessment of decellularized porcine diaphragm conjugated with gold nanomaterials as a tissue scaffold for wound healing," *J. Biomed. Mater. Res. A*, vol. 99A, no. 3, pp. 426–434, Sep. 2011.

[4] Y. Liu, G. Zhou, and Y. Cao, "Recent Progress in Cartilage Tissue Engineering—Our Experience and Future Directions," *Engineering*, vol. 3, no. 1, pp. 28–35, Feb. 2017.

[5] L. A. Castillo Diaz, M. Elsawy, A. Saiani, J. E. Gough, and A. F. Miller, "Osteogenic differentiation of human mesenchymal stem cells promotes mineralization within a biodegradable peptide hydrogel," *J. Tissue Eng.*, vol. 7, p. 204173141664978, Jan. 2016.

[6] A. R. Sun, T. Friis, S. Sekar, R. Crawford, Y. Xiao, and I. Prasadam, "Is Synovial Macrophage Activation the Inflammatory Link Between Obesity and Osteoarthritis?," *Curr. Rheumatol. Rep.*, vol. 18, no. 9, p. 57, Sep. 2016.

[7] T. J. Bartosh and J. H. Ylostalo, "Macrophage Inflammatory Assay," *Bio-Protoc.*, vol. 4, no. 14, Jul. 2014.

[8] E. L. Kuyinu, G. Narayanan, L. S. Nair, and C. T. Laurencin, "Animal models of osteoarthritis: classification, update, and measurement of outcomes," *J. Orthop. Surg.*, vol. 11, Feb. 2016.

[9] M. Drobnic, D. Radosavljevic, D. Ravnik, V. Pavlovcic, and M. Hribernik, "Comparison of four techniques for the fixation of a collagen scaffold in the human cadaveric knee," *Osteoarthritis Cartilage*, vol. 14, no. 4, pp. 337–344, Apr. 2006.

7. Appendix: Supplemental Images and Graphs

A.1 Contact Angle Images of Pristine PCL

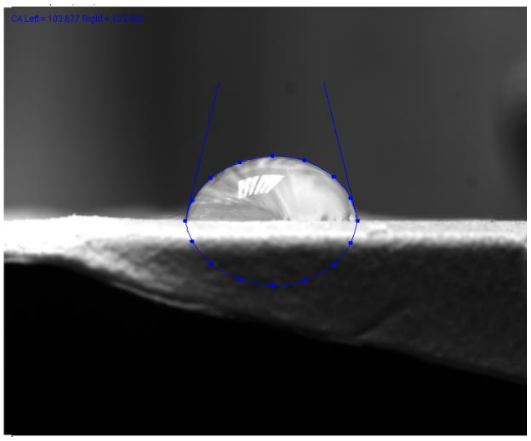

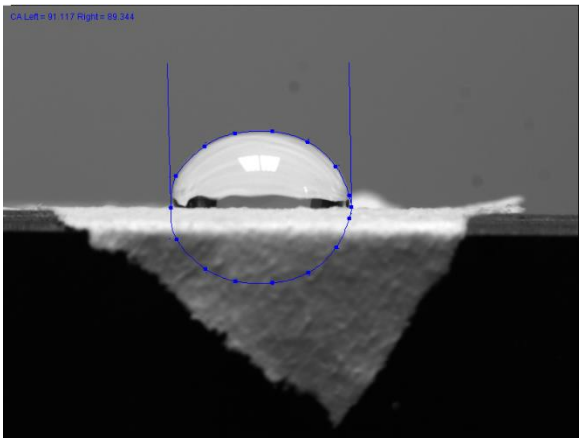

A.2 Contact Angle Image of 40:40

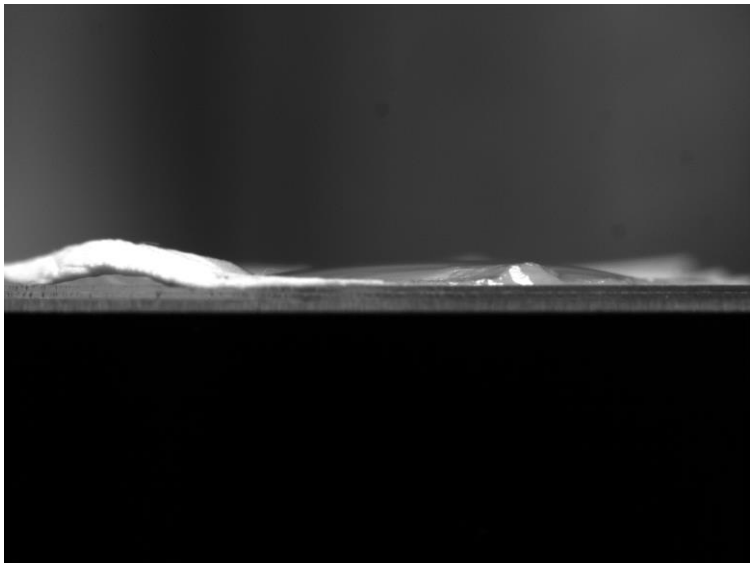

A.3 DSC Thermogram for PCL

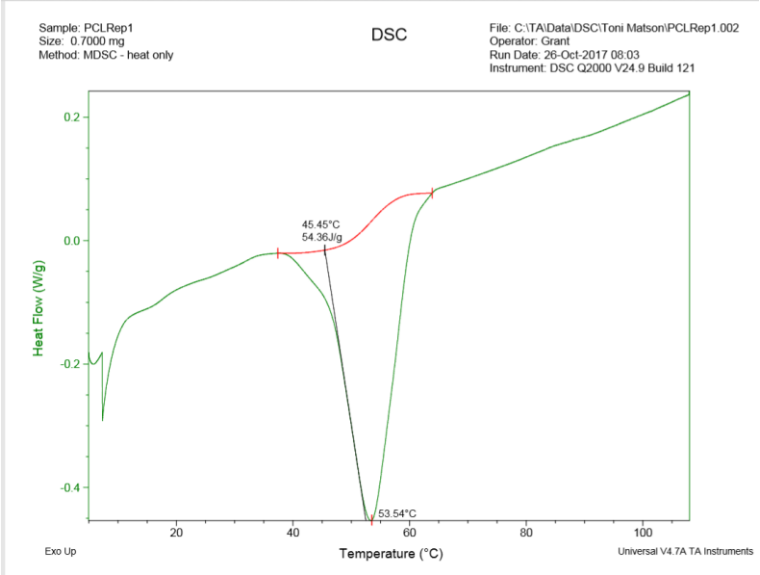

A.4 DSC Thermogram for 40:40

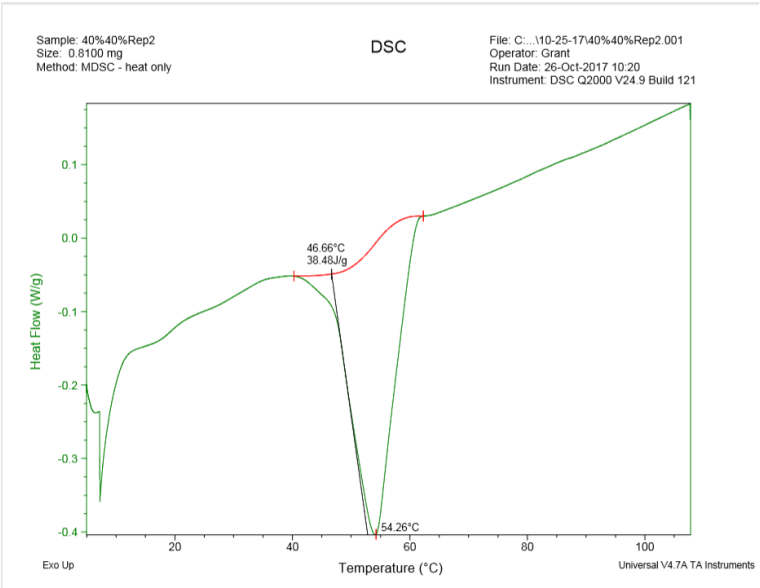

A.5 DSC Thermogram for 50:50

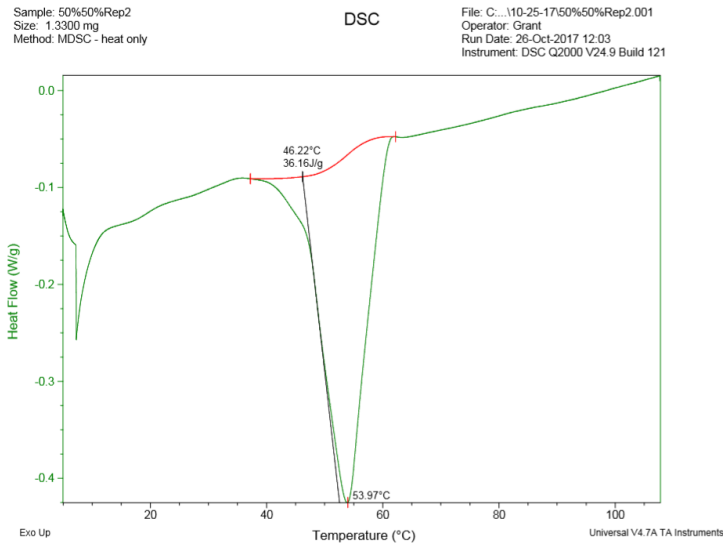

A.6 100X and 1000X magnification SEM micrographs of non-polymerized 50:50

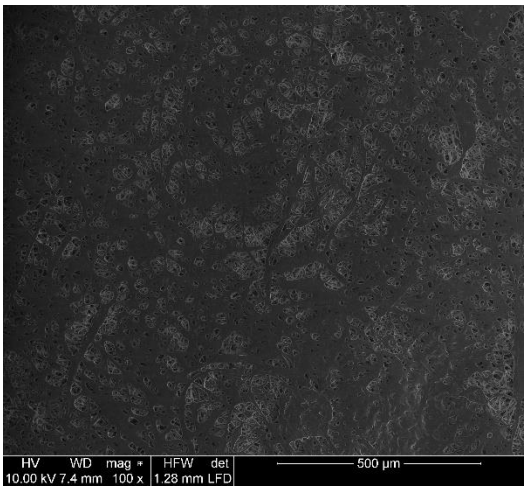

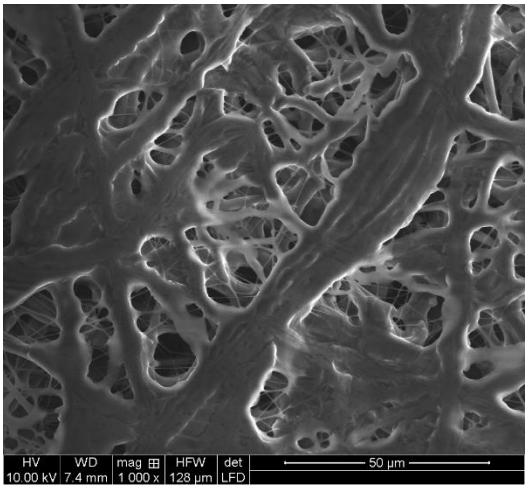

A.7 100X and 1000X magnification SEM micrographs of non-polymerized 40:40